

# **A Comparison of the Accuracy of Different Intra- and Extra-Oral Digital Scanners for Milling an Implant-Supported Framework**

**Dr M Michael**

0306489H

A research report submitted to the School of Oral Health Sciences, Faculty of Health Sciences, University of the Witwatersrand, in partial fulfilment of the requirements for the degree of Master of Dentistry in the branch of Prosthodontics

Johannesburg, 2017



## DECLARATION

I Michael Michael declare that this Research Report is my own, unaided work. It is being submitted for the Degree of Master of Dentistry in the branch of Prosthodontics at the University of the Witwatersrand, Johannesburg. It has not been submitted before for any degree or examination at any other University.



---

15 day of June 2017 in Johannesburg

## ABSTRACT

**Purpose:** To perform a comparative analysis of the accuracy of intra-oral and extra-oral digital scanners when used for the milling of a long-span implant supported superstructure framework.

**Method:** Three intra-oral and three extra-oral scanners were used to measure a master model containing five implant analogues. The three-dimension positions of the implant analogues were measured with a coordinate measuring machine. The digital data from the scanners were used to mill the implant positions in aluminium blanks from a single milling device. These implant positions were measured at the same points as the master model. The three-dimensional differences were calculated to provide a measure of the most accurate frameworks.

**Results:** For the intra-oral scanners, the further the measurement between points, the greater the standard deviation (the poorer the precision) and the poorer the mean accuracy. However, these were clinically acceptable over short distances. For the extra-oral scanners, there was no correlation between the length of the measured distances and the accuracy of the produced framework. All the extra-oral scanners were clinically acceptable for complete-arch prostheses.

**Conclusions:** Noting the limitations of this study and the use of a milling centre to mill the frameworks, for the intra-oral scanners, the 3Shape Trios® (3Shape, Copenhagen, Denmark) can be used for measurements up to 21,5mm and the Sirona CEREC OmniCam (Sirona Dental Systems, Inc., Bensheim, Germany) can be used for measurements up to 34mm.

The extra-oral scanners used in this study can be used for complete-arch implant prosthetics. The accuracy of these is relative to the model or impression created. Steps should therefore be made to ensure the accuracy of the model such as the use of a verification jig.

## **ACKNOWLEDGMENTS**

Professor CP Owen, for his mentorship, supervision, inspiration and academic guidance

Professor DG Howes, for his mentorship, encouragement, supervision and clinical insight

Mr George Sansoni (from Retecon), for his expertise in metrology and the generous use of the measuring instruments

Mr Zarius Marx (from Metal Free Dental), for his assistance in designing and milling of the required frameworks

Mr Dion van Zyl, for his expertise and guidance in the statistical analysis

Mr Chris Boschhoff (Bostech Laboratories), for the design of the soft tissue mask

Southern Implants (Irene, Pretoria), for the donation of the scan flags

## LIST OF FIGURES

		Pg
<b>Figure 3.1</b>	Digital file of the planned mill of the implant platform showing no absolute and reproducible sharp edges	7
<b>Figure 3.2</b>	Superimposition of the actual (black), and proposed (blue) fit of the implant hexagon showing a 100µm tolerance in diameter	8
<b>Figure 3.3</b>	Portable CMM, Romer Absolute Arm 7330SI with a 3mm diameter probe measuring the master model	9
<b>Figure 3.4</b>	CAD representation of the difference of levels a 3mm probe rests between and implant and a component or superstructure designed to fit on the implant platform	10
<b>Figure 3.5</b>	Three points recorded on the implant platform	11
<b>Figure 3.6</b>	Four points recorded on the outer circumference of the implant	12
<b>Figure 3.7</b>	Stationary CMM Global Classic 07.10.05 with 0.5mm diameter probe measuring the milled framework	12
<b>Figure 3.8</b>	Three points (orange) recorded on the surface corresponding to the implant platform and four points (red) recorded on the outer circumference	13
<b>Figure 3.9</b>	Master model	13
<b>Figure 3.10</b>	Digitally designed gingival mask	14
<b>Figure 3.11</b>	3D printed soft-tissue mask with scan flags	14
<b>Figure 3.12</b>	Print-screen of an intra-oral scan from the Sirona CEREC OmniCam (Sirona Dental Systems, Inc., Bensheim, Germany)	16
<b>Figure 3.13</b>	Print-screen grab of an extra-oral scan from the Sirona CEREC Inlab inEos X5 (Sirona Dental Systems, Inc., Bensheim, Germany)	16
<b>Figure 3.14</b>	Milled frameworks in aluminium blanks (ASTM B348, Acnis, Villeurbanne, France)	18
<b>Figure 3.15</b>	Representation of distances measured	19
<b>Figure 4.1</b>	Error bars of frameworks (created with the Trios® intra-oral scanner) relative to the master model at 95% confidence interval	23
<b>Figure 4.2</b>	Error bars of frameworks (created with the CS 3500 intra-oral scanner) relative to the master model at 95% confidence interval	23
<b>Figure 4.3</b>	Error bars of frameworks (created with the OmniCam intra-oral scanner) relative to the master model at 95% confidence interval	24

	<b>Pg</b>
<b>Figure 4.4</b> Error bars of frameworks (created with the D700 extra-oral scanner) relative to the master model at 95% confidence interval	26
<b>Figure 4.5</b> Error bars of frameworks (created with the inEos X5 extra-oral scanner) relative to the master model at 95% confidence interval	26
<b>Figure 4.6</b> Error bars of frameworks (created with the S600 ARTI extra-oral scanner) relative to the master model at 95% confidence interval	27
<b>Figure 4.7</b> Error bars of frameworks (created with the grouping intra-oral scanners) relative to the master model at 95% confidence interval	29
<b>Figure 4.8</b> Error bars of frameworks (created with grouping of extra-oral scanners) relative to the master model at 95% confidence interval	29
<b>Figure 4.9</b> Error bars of frameworks created with individual scanners using the mean sum of all measurements relative to the master model at 95% confidence interval	30
<b>Figure 4.10</b> Error bars of frameworks created with the intra-oral group of scanners and the extra-oral group of scanners using the mean sum of all measurements relative to the master model at 95% confidence interval	32

## LIST OF TABLES

		<b>Pg</b>
<b>Table 1.</b>	Three dimensional measurements for each distance on each experiment and differences of these to the master model	21
<b>Table 2.</b>	t-test of the absolute differences (and the mean sum of the differences) of milled frameworks made by individual intra-oral scanners relative to the master model	22
<b>Table 3.</b>	t-test of the absolute differences (and the mean sum of the differences) of milled frameworks made by individual extra-oral scanners relative to the master model	25
<b>Table 4.</b>	t-test of the absolute differences (and the mean sum of the differences) of milled frameworks made by the group of intra-oral scanners and the group of extra-oral scanners relative to the master model	28
<b>Table 5.</b>	t-test comparing intra-oral with extra-oral scanners using the absolute differences of milled frameworks relative to the master model	31

<b>Contents</b>	<b>Page</b>
<b>DECLARATION</b> .....	<b>I</b>
<b>ABSTRACT</b> .....	<b>II</b>
<b>ACKNOWLEDGMENTS</b> .....	<b>III</b>
<b>LIST OF FIGURES</b> .....	<b>IV</b>
<b>LIST OF TABLES</b> .....	<b>VI</b>
<b>CHAPTER 1. INTRODUCTION AND LITERATURE REVIEW</b> .....	<b>1</b>
<b>CHAPTER 2. AIMS AND OBJECTIVES</b> .....	<b>5</b>
2.1    AIM.....	5
2.2    OBJECTIVES .....	5
<b>CHAPTER 3. MATERIALS AND METHODS</b> .....	<b>6</b>
3.1    SAMPLE SIZE .....	6
3.2    ACCURACY OF MEASUREMENT.....	6
3.2.1 <i>The Reflex Microscope</i> .....	6
3.2.2 <i>Coordinate Measuring</i> .....	8
3.3    MATERIALS AND METHODS.....	13
3.4    DATA ANALYSIS .....	19
<b>CHAPTER 4. RESULTS</b> .....	<b>20</b>
<b>CHAPTER 5. DISCUSSION</b> .....	<b>33</b>
5.1    DISCUSSION .....	33
5.2    STUDY LIMITATIONS .....	36
<b>CHAPTER 6. CONCLUSION AND RECOMMENDATIONS</b> .....	<b>37</b>
<b>REFERENCES</b> .....	<b>39</b>
7.1    CITED REFERENCES .....	40
<b>APPENDICES</b> .....	<b>41</b>

## CHAPTER 1. INTRODUCTION AND LITERATURE REVIEW

Dental implants have been used to provide support for fixed prostheses in edentulous jaws since 1965 (Brånemark, 2005), and longitudinal studies have proven the effectiveness of this treatment modality (Adell et al., 1981; Ekelund et al., 2003; Astrand et al., 2008; Turkyilmaz & Tözüm, 2015). The focus of these studies was mainly on the survival of the implants and associated rehabilitation. However, throughout the lifespan of any dental rehabilitation, biologic and technical complications can be expected. Reports on these complication rates in complete-arch implant-supported prostheses (ISP) have shown that technical complications occur more commonly than biological complications (Papaspolidakos et al., 2012). This may be due to the mechanical nature of a prosthesis supported by dental implants that are essentially ankylosed within the bone. This configuration allows for less recognition of and hence biological tolerance of, the functional and parafunctional forces generated compared with tooth-supported prostheses (Kim et al., 2005). This can lead to a higher distribution of forces within the prosthetic assembly.

The fit of the prosthetic superstructure framework has also been implicated in the additional generation of forces prior to functional loading. Reducing these pre-functional forces by attempting to achieve a “passive fit” has been said to reduce both biologic and technical complications (Zarb & Schmitt, 1990; Sahin & Cehreli, 2001; Abduo, 2014). There is a lack of high level evidence to make this association, particularly since passivity cannot be accurately measured *in vivo*. However, until guidelines on passive fit for ISPs are developed, it is crucial to aim for the best possible fit to minimise strain and gap formation. Various authors have proposed a degree of accuracy that ISPs should aim to achieve. Brånemark (1983) suggested a fit of 10µm or less between the prosthetic framework and implant

abutment. Jemt (1991) suggested that a misfit of up to 150µm was acceptable and this seems to have been widely accepted (Mitha et al., 2009).

The fabrication of an ISP requires multiple clinical and laboratory steps involving a variety of materials. The techniques employed and the inherent inaccuracies of the materials can result in cumulative dimensional changes resulting in a misfit of the fabricated ISP (Mitha et al., 2009; Hoods-Moonsammy et al., 2014). Traditional steps include impression making, pouring a master cast and waxing, investing, and casting a framework. Furthermore, the dimensional stability over time of plaster casts is not known. These casts may be useful for the lifetime of the patient.

With improved knowledge and technology, a number of approaches have been proposed to improve the fit of ISPs. A recent review on failure and complication rates in ISPs showed an improvement of outcomes in studies published in the last decade compared with prior studies (Pjetursson et al., 2014). This may partly be due to two different approaches, 1) the addition of fit refinement steps and 2) the elimination of fabrication steps. The first category includes techniques such as sectioning and soldering / laser welding frameworks. The second category includes computer-aided design/computer-assisted manufacturing (CAD/CAM) (Abduo et al., 2011). In their review, Abduo et al. (2011) concluded that CAD/CAM was able to provide the most consistent outcome.

The workflow of intra-oral digital impressions compared with traditional impressions eliminates the potential inaccuracies that may arise from the impression material itself, the

pouring of a cast and fabricating a prosthesis. The workflow of extra-oral digital impressions eliminates the potential inaccuracies that may arise from prosthesis fabrication only.

There have been very few studies assessing intra-oral scanners for complete-arch ISPs. These studies have used different methodologies, but none have assessed the entire pathway measuring a milled product and none have compared intra-oral scanners with extra-oral scanners.

Vandeweghe et al. (2016) assessed the accuracy of four different intra-oral scanners used for complete-arch ISPs. The master model comprised six implants within an acrylic mandibular cast. Measurements were done digitally using metrology software. To obtain a digital file of the master model, the acrylic cast was scanned with an extra-oral scanner. Therefore, all errors and measurements were relative to the extra-oral scan. This was not a true reflection of the master model.

Katsoulis et al. (2015) assessed and compared the precision of fit of long-span (six implants, ten units) with short-span (three implants, five units) CAD/CAM ISPs. An extra-oral scanner was used for the pathway of fabrication. The method of measurements was the “one-screw test” and scanning electron microscope (SEM) measurements of the vertical misfit along the remaining implants. The conclusion was that all ISPs were within clinical limits, with the short-span ISPs being more accurate. The method of measurement did not take into account a three-dimensional misfit. A horizontal misfit may result in a poor alignment of the ISP screw access channel to the implant fixture.

As no studies have been found to determine the accuracy of scanners or to compare intra-oral with extra-oral scanners, this study was designed as an *in vitro* comparative analysis of the ability of three intra-oral scanners and three extra-oral scanners to accurately record the positions of a 5-implant model in three dimensions when their scanned data are used to mill a superstructure framework.

## **CHAPTER 2. AIMS AND OBJECTIVES**

### **2.1 Aim**

To determine and compare the accuracy of the digital pathway from scanning to milling with which 3 intra-oral and 3 extra-oral scanners can replicate implant positions from a stainless-steel master model containing five implant analogues.

### **2.2 Objectives**

1. To determine the most accurate method of measuring the implant and milled positions of the implant fixtures in three dimensions.
2. To measure in three-dimensions the implant positions of the stainless-steel master model and the equivalent positions on the resultant milled aluminium frameworks.
3. To determine, for each scanner, whether the mean differences between the master model and the milled blank are significantly different from zero.
4. To compare the mean differences within each scanner type and between the different types of scanners.

### **2.3 Null Hypothesis**

The null hypothesis is that there would be no difference in the accuracy of different scanning methods.

## **CHAPTER 3. MATERIALS AND METHODS**

### **3.1 Sample Size**

Sample size determination was based on the key research question, namely the determination of between-scanner differences. It was decided to use a between-group difference (in the master vs. milled framework dimension differences) of 110 $\mu\text{m}$ , as this is within the 150 $\mu\text{m}$  of Jemt's (1991) recommendations. Based on this, a within-group standard deviation of 1.5 $\mu\text{m}$  (based on a 15% relative standard deviation of a difference of 10 $\mu\text{m}$ ), 80% power and the 5% significance level, a samples size of two per group was required. This was increased to 3 samples per group for practical considerations (e.g. in case of experimental losses).

### **3.2 Accuracy of Measurement**

The accuracy of the measurement method has an influence on the results and thus the outcomes of the study. Careful consideration of the choice of measuring tools, the digital pathway for prosthesis design, and the milling limitations was necessary to establish an appropriate study design.

#### **3.2.1 The Reflex Microscope**

A reflex microscope was considered, but the circumference of the milling bur precludes a sharp edge being formed. A sharp edge is necessary to determine a reproducible point between all samples to be measured, which is required for the accurate positioning of the light source point in the reflex microscope. This also precluded correlation with the master model. This is seen in the CAD diagram below of the implant fitting surface of the framework.

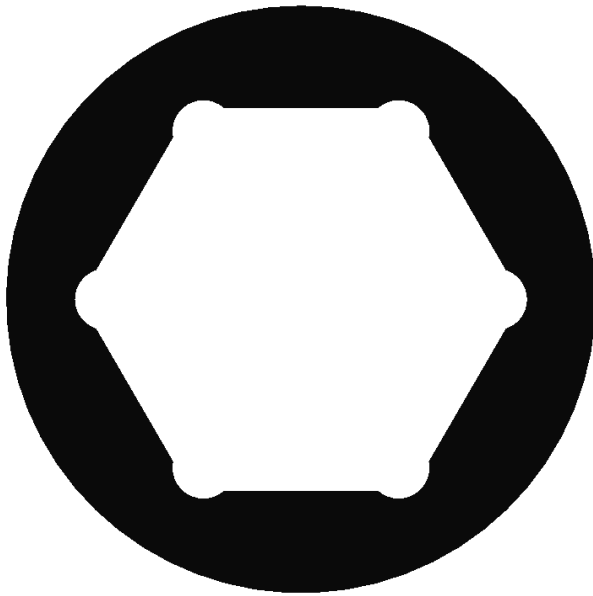


**Figure 3.1** Digital file of the planned mill of the implant platform showing no absolute and reproducible sharp edges

Because of inaccuracies which occur with CAD/CAM pathways in implant-supported prosthesis fabrication, implant companies build in a tolerance to the design of the fitting surface to ensure fit. The tolerance with the external hexagon implant requires a larger fitting surface over the hexagon to allow for the seating of the prosthetic platform to the implant platform. This information is transferred during the design process when correlating the scan flag to implant position. The imported information of the fitting surface is, therefore, different from the actual implant. Below is the CAD representation of the above description. The proposed fit is superimposed onto the actual size of the hexagon. Southern Implants (Irene, South Africa) have incorporated 100 $\mu$ m of tolerance as seen below.

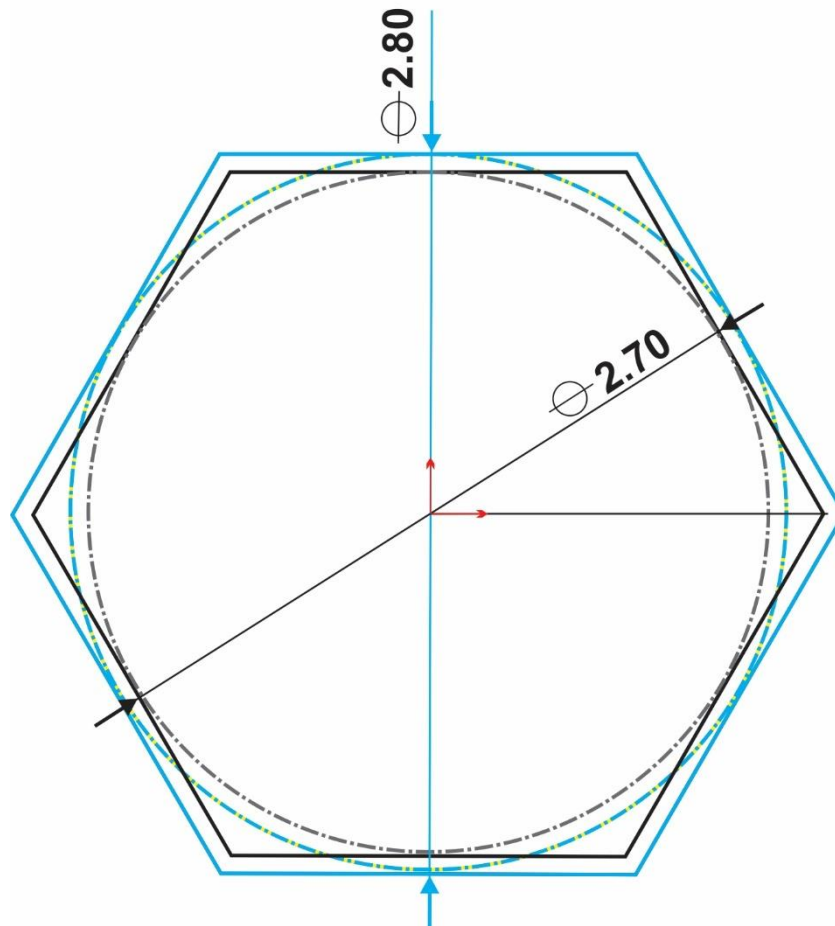


**Figure 3.2** Superimposition of the actual (black), and proposed (blue) fit of the implant hexagon showing a 100µm tolerance in diameter

### 3.2.2 Coordinate Measuring

The only appropriate way of correlating a CAD/CAM framework to a master model is finding the centre point at a corresponding level. This centre point cannot be determined by a reflex microscope. Therefore, the measuring tool of choice is a coordinate measuring machine (CMM). CMMs are either portable or stationary. Both varieties work by plotting the X, Y and Z coordinates of chosen points via a laser arm and probe.

Portable CMMs use movable arms which are operator controlled. This introduces potential for operator error. Furthermore, the accuracy of portable CMMs is less than the stationary type which is computer numerically controlled (CNC). A portable CMM, the Romer Absolute Arm 7330SI (Hexagon Manufacturing Intelligence (HexagonMI), Surrey, Great Britain), was tried, as it had been used in previous research (Hoods-Moonsammy et al., 2014). A 3mm probe (Fig. 3) sits on the implant fixture, and the coordinates of the centre of the probe are recorded via computer software. The manufacturer specifies the scanning system accuracy of this arm to be 119 $\mu$ m.

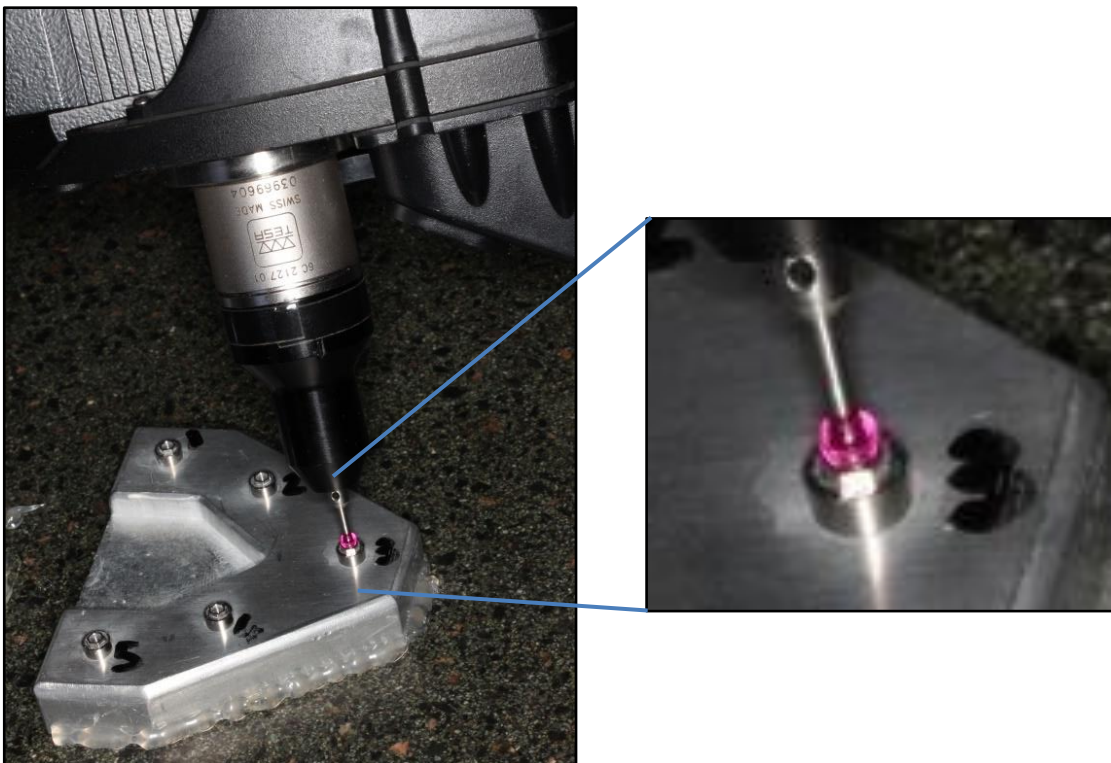


**Figure 3.3** Portable CMM, Romer Absolute Arm 7330SI with a 3mm diameter probe measuring the master model

Due to the differing geometry of the implant platform, and any component or superstructure designed to fit on the implant platform, the position of the probe can differ. On the implant, the 3mm probe will rest on the elevated hexagonal orientation. This is raised 0.7mm from the outer platform. On componentry designed to fit the implant, the 3mm probe rests on the outer

platform. Because the probe rests over a cylindrical opening in both instances, the wider the diameter of the opening, the deeper the probe will rest. Since the diameters vary, the probe rests at different levels. This creates further discrepancies. This is illustrated in figure 3.4.

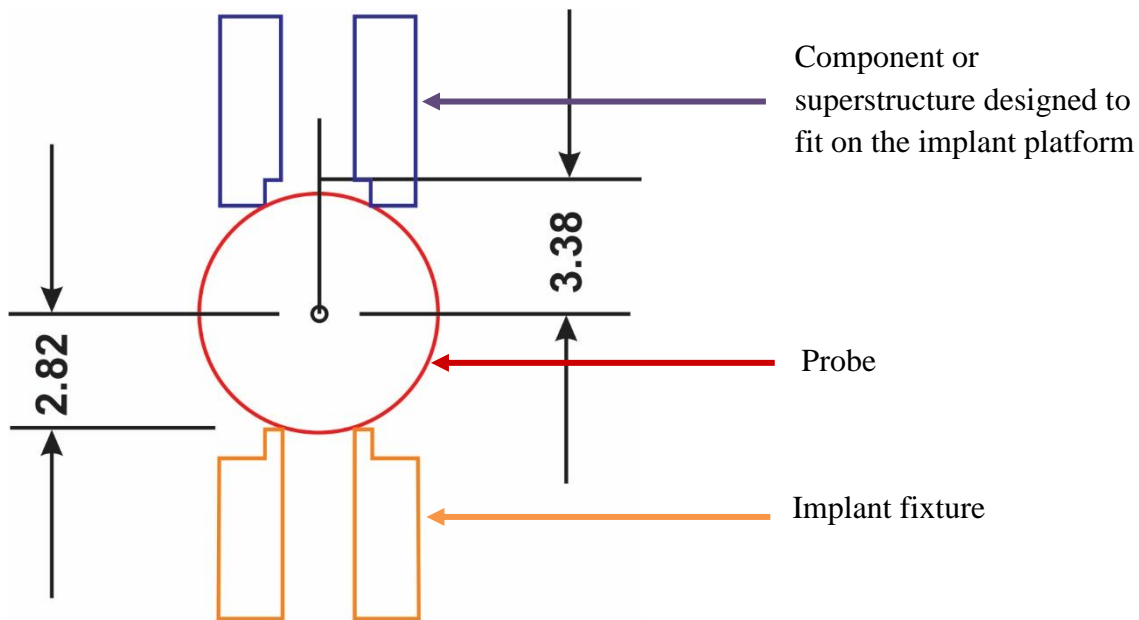


**Figure 3.4** CAD representation of the difference of levels a 3mm probe rests between and implant and a component or superstructure designed to fit on the implant platform

From the CAD illustration above, the probe rests 2.82mm above the implant but 3.38mm above componentry designed to fit over the implant at the corresponding level. This creates a difference of 560µm, assuming the arm is completely accurate, which it is not, as its specified (in)accuracy is 119µm Therefore this method of measurement is inappropriate.

It was therefore necessary to use a stationary CMM, in this case the Global Classic 07.10.05 (Hexagon Manufacturing Intelligence, Surrey, Great Britain) was used. The accuracy is described by the manufacturer as the Maximum Permissible Error (MPE<sub>E</sub>), defined as  $MPE_E(\mu m) = 2.5 + L/300$  where L is the measurement length in millimetres. This means that

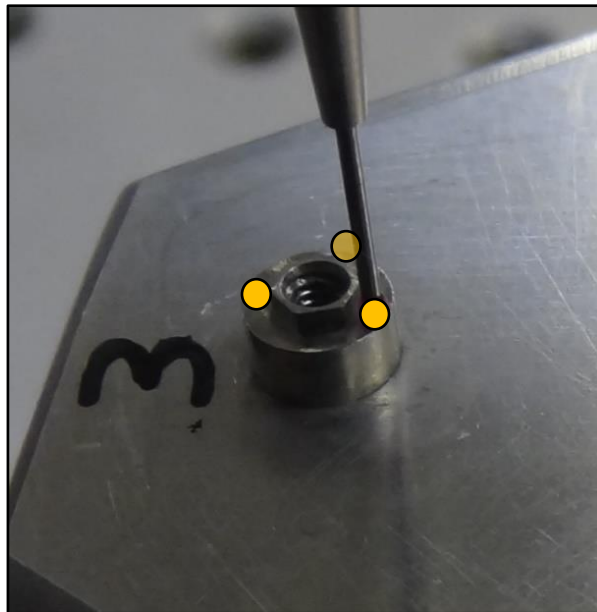
the greater the distance measured, the greater the permissible error range. In this study the smallest measurement was 21.355mm and the largest measurement was 50.876mm.

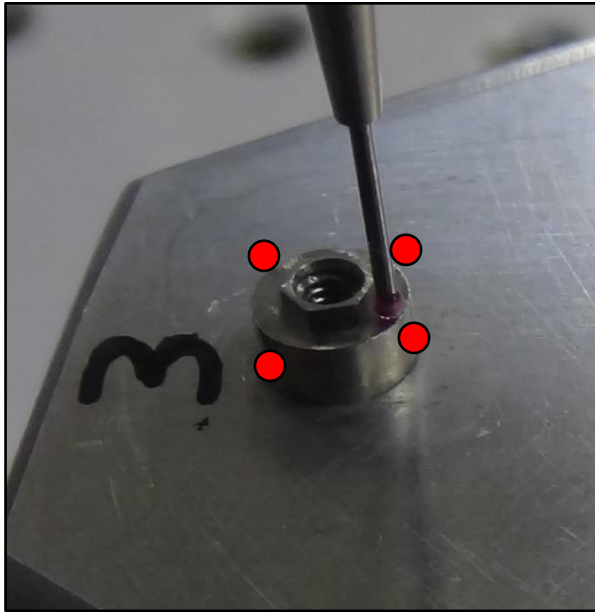
Therefore, the range of accuracy of the study can be calculated as follows:

$$\begin{aligned} \text{MPE}_E &= 2.5 + 21.355/300 & \text{to} & & \text{MPE}_E &= 2.5 + 50.876/300 \\ &= 2.571\mu\text{m} & & & &= 2.669\mu\text{m} \end{aligned}$$

The probe selection was also key to obtaining the centre of the implant at the platform level. A probe with 0.5mm diameter was chosen. This probe is controlled by computer via CNC software after the CAD drawings of the proposed object are imported. The probe records seven points for each implant fixture or implant fixture fitting surface, as seen below in figures 3.5 and 3.6. Three points are recorded at the implant platform (figure 3.5) to determine the orientation and level of the platform, and four points are recorded at the outer circumference (figure 3.6).

**Figure 3.5** Three points recorded on the implant platform

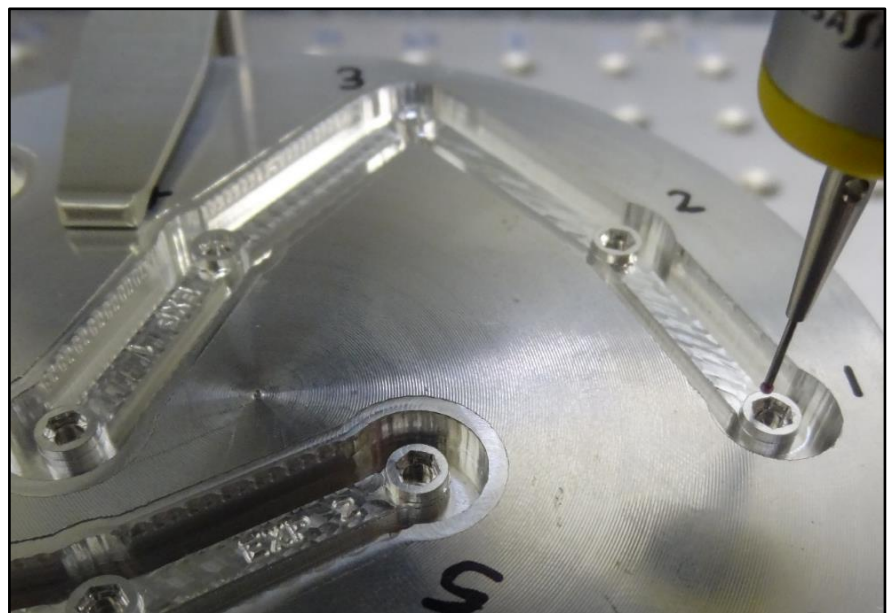




**Figure 3.6** Four points recorded on the outer circumference of the implant fixture

The probe touches a single point and records the coordinates of that point by calculating the known radius of the probe to that point. The points recording the outer circumference are connected digitally to form the circular shape. The centre of this circle is then determined by the software at the level of the platform. The same process occurs for the each of the milled frameworks. This is seen below in figures 3.7 and 3.8.

**Figure 3.7** Stationary CMM Global Classic 07.10.05 with 0.5mm diameter probe measuring the milled framework



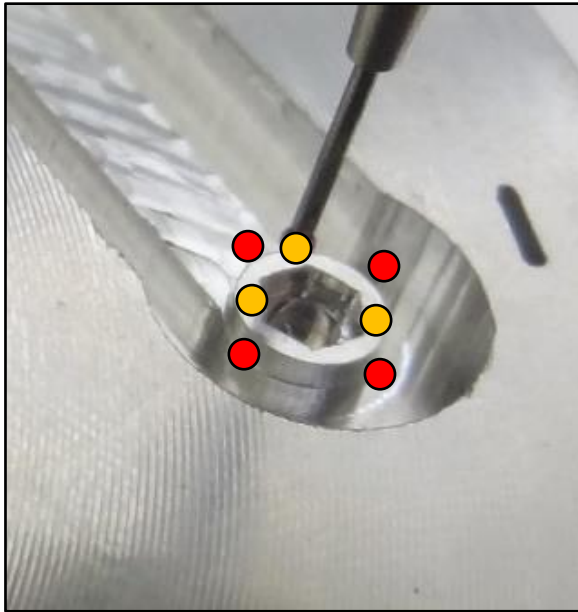


**Figure 3.8** Three points (orange) recorded on the surface corresponding to the implant platform and four points (red) recorded on the outer circumference

### 3.3 Materials and methods

A stainless-steel master model was made available which had been prepared to mimic a dental arch containing five implant analogues (Southern Implants, Irene, South Africa) (figure 3.9).

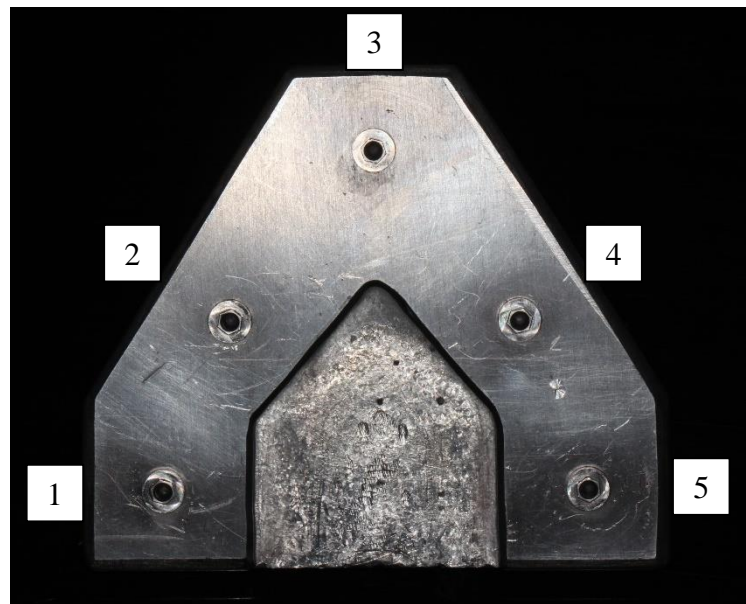


**Figure 3.9** Master model

Digitally designed and printed soft tissue was designed to seat over the model to mimic the typical intra-oral anatomy of an edentulous maxilla (figures 3.10 and 3.11). This is important for the scanning process to be effective as multiple images are stitched together while acquiring the scan. This is particularly crucial with intra-oral scanners which have one camera which is moved across the desired area to be scanned.

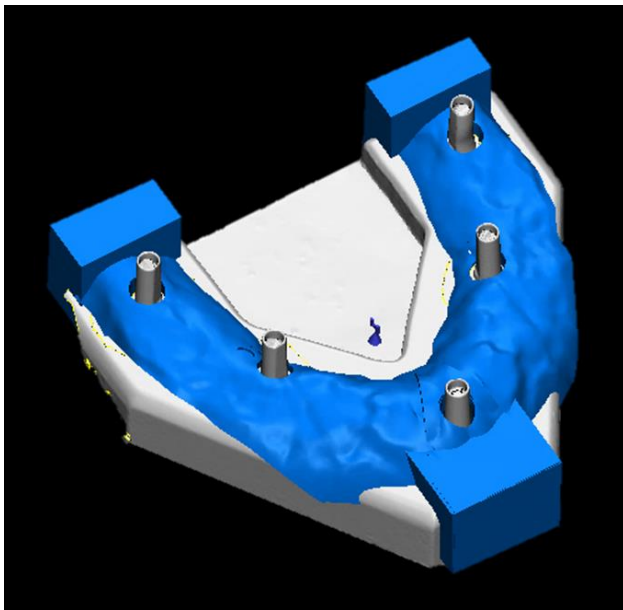


**Figure 3.10** Digitally designed gingival mask



**Figure 3.11** 3D printed soft-tissue mask with scan flags

Five impression scan flags (Southern Implants, Irene, South Africa) were used during scanning (the same five scan flags were used for all the digital scans). These are seen in figure 3.11. The scan flags were torqued to 10Ncm onto the implant analogues as per the manufacturer's instructions.

The master model, with the printed soft tissue mask, and scan flags was scanned three times per scanner. The following scanners were used:

Intra-oral scanners:

3Shape Trios® (3Shape, Copenhagen, Denmark)

Carestream CS3500 (Rochester, New York, United States of America)

Sirona CEREC OmniCam (Sirona Dental Systems, Inc., Bensheim, Germany)

Extra-oral scanners:

3Shape D700 (3Shape, Copenhagen, Denmark)

Sirona CEREC Inlab inEos X5 (Sirona Dental Systems, Inc., Bensheim, Germany)

Zirkonzhan Scanner S600 ARTI (Zirkonzhan, Gais, Italy)

Examples of an intra-oral scan and an extra-oral scan are seen in figures 3.12 and 3.13 respectively.



**Figure 3.12** Print-screen of an intra-oral scan from the Sirona CEREC OmniCam (Sirona Dental Systems, Inc., Bensheim, Germany)

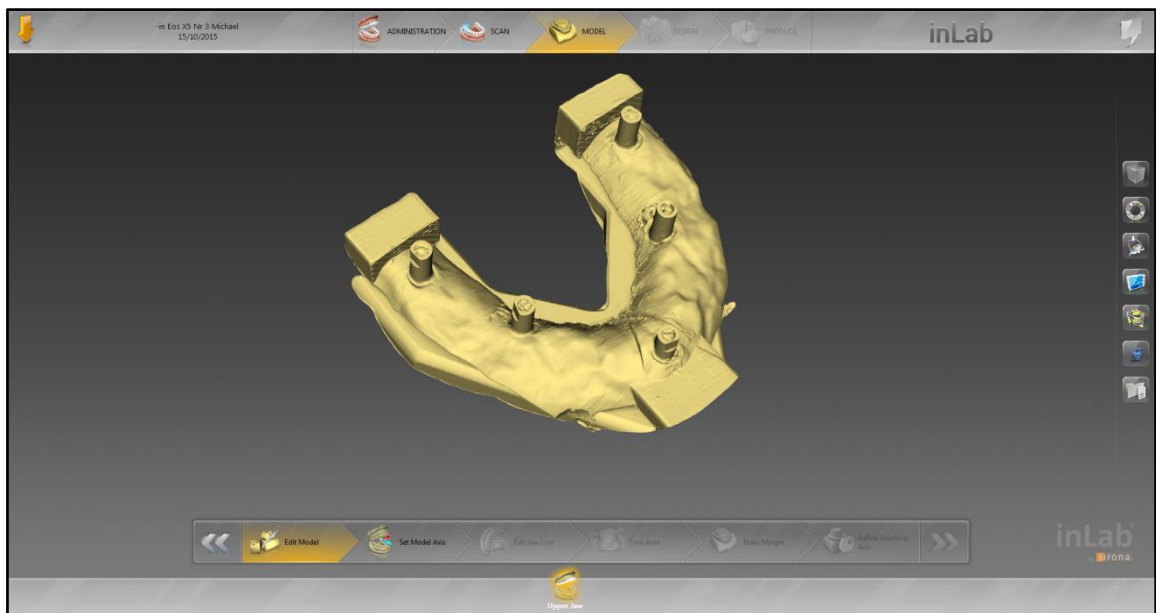


**Figure 3.13** Print-screen grab of an extra-oral scan from the Sirona CEREC Inlab inEos X5 (Sirona Dental Systems, Inc., Bensheim, Germany)

This digital information was converted into Standard Tessellation Language (.stl) format by each scanner's software, where necessary. These .stl files were exported into Dental System™ (3Shape, Copenhagen, Denmark) CAD software for the design process. The scans were labelled as experiments (EXP) as follows:

3Shape Trios®: EXP 1 – EXP 3

Carestream CS3500: EXP 4 – EXP 6

Sirona CEREC OmniCam: EXP 7 – EXP 9

3Shape D700: EXP 10 – EXP 12

Sirona CEREC Inlab inEos X5: EXP 13 – EXP 15

Zirkonzhan Scanner S600 ARTI: EXP 16 – EXP 18

This was done to blind the software engineer designing the frameworks from the scanners from knowing the origin of each file. The digital files of the scan flags were used to transfer information of implant position using Dental System™ (3Shape, Copenhagen, Denmark) CAD software. Identical frameworks were then designed to link the implant positions along the mimicked arch using the software. These were then milled using a single milling unit (D40, Yenadental, Istanbul, Turkey) to mill the implant positions in the aluminium blanks (ASTM B348, Acnis, Villeurbanne, France). To identify the frameworks, each framework had its experiment number milled into it. Figure 3.14 is an example of how the frameworks were designed and milled.



**Figure 3.14** Milled frameworks in aluminium blanks (ASTM B348, Acnis, Villeurbanne, France)

The coordinate measuring machine data were documented on a computer via a direct link with the use of computer software (PolyWorks®, InnovMetric Software Inc., Quebec, Canada). The documented accuracy of the specific CMM used is within  $3\mu\text{m}$  of accuracy (Hexagonmi, n.d.).

All scans, milling and measurements were done in controlled environments at  $21^\circ\text{C}$ .

Ten distances (1-2, 1-3, 1-4, 1-5, 2-3, 2-4, 2-5, 3-4, 3-5, 4-5) (Fig. 3.15) were calculated using the PolyWorks® software. Representation of these distances is seen in the figure below.

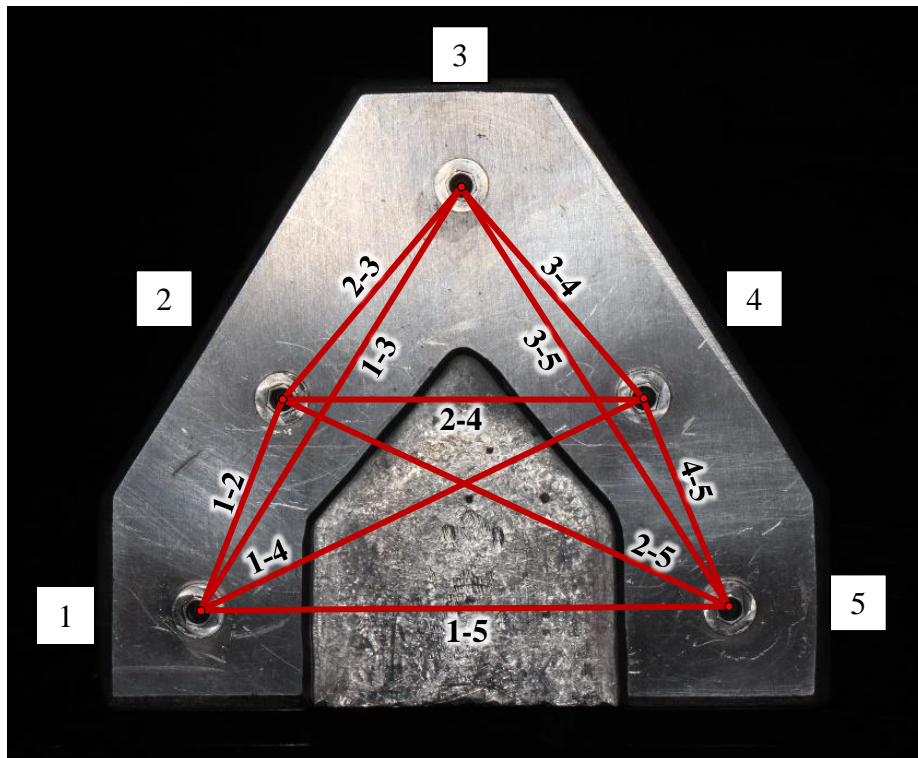


**Figure 3.15** Representation of distances measured

### **3.4 Data analysis**

Data was entered into an Excel® (Microsoft Corporation) spreadsheet in preparation for analysis. Data analysis was carried out in IBM® SPSS® Statistics Version 24 (IBM Corporation). For each experiment, the difference in each dimension between the master model and the milled implant positions was calculated. These were the outcome variables which were used in the data analysis. The analysis followed a two-step process. Firstly, descriptive statistics were calculated including mean values (i.e. mean difference from zero) and standard deviations. Secondly, for each dimension and for each scanner, the mean differences were tested for significant differences to zero (one-sample t-test). The means of differences were also calculated and tested.

## CHAPTER 4. RESULTS

The raw data of the measurements and the differences of these measurements to the master model are found in Table 1. The differences (“Diff\_” in the figures) are converted to absolute values relative to zero, zero being the measurements from the master model. Table 2 shows the mean values and t-test for the intra-oral scanners for each measurement and the mean sum of each measurement relative to the master model. Table 2 is accompanied by graphic representation of these results in figures 4.1-4.3. Table 3 shows the mean values and t-test for the extra-oral scanners for each measurement and the mean sum of each measurement relative to the master model. Table 3 is accompanied by graphic representation of these results in figures 4.4-4.6. Table 4, with accompanying figures 4.7-4.9, reflect the t-tests grouping all the intra-oral scanners together and all the extra-oral scanners together relative to the master model. Table 5 shows t-tests of the group of intra-oral scanners relative to the group of extra-oral scanners, represented on figure 4.10.

Units	Object	Control	Master Model	Measurement Results Actual to Nominal Master Model																	
				EXP 1	EXP 2	EXP 3	EXP 4	EXP 5	EXP 6	EXP 7	EXP 8	EXP 9	EXP 10	EXP 11	EXP 12	EXP 13	EXP 14	EXP 15	EXP 16	EXP 17	EXP 18
mm	distance 1-2	3D Distance	21.541	21.572	21.537	21.566	21.527	21.537	21.572	21.520	21.559	21.531	21.512	21.462	21.520	21.582	21.559	21.520	21.564	21.550	21.611
mm	distance 1-3	3D Distance	47.168	47.307	47.201	47.296	46.998	47.263	47.242	47.260	47.104	47.058	47.091	47.108	47.128	47.165	47.174	47.121	47.194	47.080	47.793
mm	distance 1-4	3D Distance	46.522	46.647	46.871	46.833	46.285	46.546	46.489	46.589	46.490	46.487	46.454	46.432	46.449	46.518	46.553	46.550	46.523	46.501	46.939
mm	distance 1-5	3D Distance	49.998	50.261	50.876	50.612	50.183	50.444	49.912	50.167	50.021	50.027	49.988	49.990	49.997	50.043	50.058	50.072	49.944	50.033	49.813
mm	distance 2-3	3D Distance	26.247	26.333	26.254	26.317	26.068	26.335	26.273	26.344	26.158	26.137	26.179	26.237	26.200	26.197	26.220	26.207	26.231	26.146	26.836
mm	distance 2-4	3D Distance	34.007	34.062	34.254	34.178	33.776	34.034	33.937	34.049	33.981	33.984	33.956	33.924	33.912	33.968	33.982	34.013	33.987	33.998	34.402
mm	distance 2-5	3D Distance	46.522	46.682	47.098	46.870	46.552	46.862	46.428	46.620	46.542	46.539	46.500	46.458	46.474	46.524	46.502	46.531	46.458	46.544	46.493
mm	distance 3-4	3D Distance	26.254	26.375	26.395	26.366	26.248	26.375	26.326	26.335	26.299	26.293	26.348	26.313	26.323	26.263	26.265	26.278	26.365	26.282	26.407
mm	distance 3-5	3D Distance	47.171	47.362	47.415	47.353	47.076	47.403	47.239	47.287	47.203	47.189	47.240	47.202	47.238	47.169	47.158	47.164	47.248	47.162	47.390
mm	distance 4-5	3D Distance	21.539	21.586	21.586	21.574	21.355	21.568	21.532	21.554	21.523	21.519	21.509	21.493	21.523	21.516	21.510	21.507	21.515	21.501	21.694

Units	Object	Control	Master Model	Measurement Deviations of Actual to Master Model																	
				EXP 1	EXP 2	EXP 3	EXP 4	EXP 5	EXP 6	EXP 7	EXP 8	EXP 9	EXP 10	EXP 11	EXP 12	EXP 13	EXP 14	EXP 15	EXP 16	EXP 17	EXP 18
mm	distance 1-2	3D Distance	21.541	0.031	-0.004	0.025	-0.014	-0.004	0.031	-0.021	0.018	-0.010	-0.029	-0.079	-0.021	0.041	0.018	-0.021	0.023	0.009	0.070
mm	distance 1-3	3D Distance	47.168	0.139	0.033	0.128	-0.170	0.095	0.074	0.092	-0.064	-0.110	-0.077	-0.060	-0.040	-0.003	0.006	-0.047	0.026	-0.088	0.625
mm	distance 1-4	3D Distance	46.522	0.125	0.349	0.311	-0.237	0.024	-0.033	0.067	-0.032	-0.035	-0.068	-0.090	-0.073	-0.004	0.031	0.028	0.001	-0.021	0.417
mm	distance 1-5	3D Distance	49.998	0.263	0.878	0.614	0.185	0.446	-0.086	0.169	0.023	0.029	-0.010	-0.008	-0.001	0.045	0.060	0.074	-0.054	0.035	-0.185
mm	distance 2-3	3D Distance	26.247	0.086	0.007	0.070	-0.179	0.088	0.026	0.097	-0.089	-0.110	-0.068	-0.010	-0.047	-0.050	-0.027	-0.040	-0.016	-0.101	0.589
mm	distance 2-4	3D Distance	34.007	0.055	0.247	0.171	-0.231	0.027	-0.070	0.042	-0.026	-0.023	-0.051	-0.083	-0.095	-0.039	-0.025	0.006	-0.020	-0.009	0.395
mm	distance 2-5	3D Distance	46.522	0.160	0.576	0.348	0.030	0.340	-0.094	0.098	0.020	0.017	-0.022	-0.064	-0.048	0.002	-0.020	0.009	-0.064	0.022	-0.029
mm	distance 3-4	3D Distance	26.254	0.121	0.141	0.112	-0.006	0.121	0.072	0.081	0.045	0.039	0.094	0.059	0.069	0.009	0.011	0.024	0.111	0.028	0.153
mm	distance 3-5	3D Distance	47.171	0.191	0.244	0.182	-0.095	0.232	0.068	0.116	0.032	0.018	0.069	0.031	0.067	-0.002	-0.013	-0.007	0.077	-0.009	0.219
mm	distance 4-5	3D Distance	21.539	0.047	0.047	0.035	-0.184	0.029	-0.007	0.015	-0.016	-0.020	-0.030	-0.046	-0.016	-0.023	-0.029	-0.032	-0.024	-0.038	0.155

Min	0.031	0.004	0.025	0.006	0.004	0.007	0.015	0.016	0.010	0.010	0.008	0.001	0.002	0.006	0.006	0.001	0.009			0.029			
Max	0.263	0.878	0.614	0.237	0.446	0.094	0.169	0.089	0.110	0.094	0.090	0.095	0.050	0.060	0.074	0.111	0.101			0.625			
Mean	0.122	0.253	0.200	0.133	0.141	0.056	0.080	0.037	0.041	0.052	0.053	0.048	0.022	0.024	0.029	0.042	0.036			0.284			
	0.192			0.110			0.053			0.051			0.025			0.039							
	0.118																		0.038				

**Table 1.** Three dimensional measurements for each distance on each experiment and differences of these to the master model.

Blue represents accuracy within 10µm

Group	Scanner	Distance	n	Mean	Min	Max	Std. Deviation	t	df	p-value	H0: Mean = 0	Effect size
Intra	Trios	Diff_1_2	3	0.0200	0.0040	0.0310	0.0142	2.443	2	0.135	Supported	1.41
		Diff_1_3	3	0.1000	0.0330	0.1390	0.0583	2.972	2	0.097	Supported	1.72
		Diff_1_4	3	0.2617	0.1250	0.3490	0.1199	3.781	2	0.063	Supported	2.18
		Diff_1_5	3	0.5850	0.2630	0.8780	0.3085	3.284	2	0.082	Supported	1.90
		Diff_2_3	3	0.0543	0.0070	0.0860	0.0418	2.253	2	0.153	Supported	1.30
		Diff_2_4	3	0.1577	0.0550	0.2470	0.0967	2.824	2	0.106	Supported	1.63
		Diff_2_5	3	0.3613	0.1600	0.5760	0.2083	3.004	2	0.095	Supported	1.73
		Diff_3_4	3	0.1247	0.1120	0.1410	0.0148	14.547	2	0.005	Not supported	8.40
		Diff_3_5	3	0.2057	0.1820	0.2440	0.0335	10.633	2	0.009	Not supported	6.14
		Diff_4_5	3	0.0430	0.0350	0.0470	0.0069	10.750	2	0.009	Not supported	6.21
		Diff_sum	3	1.9133	1.2180	2.5260	0.6579	5.037	2	0.037	Not supported	2.91
		Diff_mean	3	0.1913	0.1218	0.2526	0.0658	5.037	2	0.037	Not supported	2.91
	CS 3500	Diff_1_2	3	0.0163	0.0040	0.0310	0.0137	2.072	2	0.174	Supported	1.20
		Diff_1_3	3	0.1130	0.0740	0.1700	0.0505	3.878	2	0.061	Supported	2.24
		Diff_1_4	3	0.0980	0.0240	0.2370	0.1205	1.409	2	0.294	Supported	0.81
		Diff_1_5	3	0.2390	0.0860	0.4460	0.1860	2.226	2	0.156	Supported	1.29
		Diff_2_3	3	0.0977	0.0260	0.1790	0.0770	2.198	2	0.159	Supported	1.27
		Diff_2_4	3	0.1093	0.0270	0.2310	0.1075	1.761	2	0.220	Supported	1.02
		Diff_2_5	3	0.1547	0.0300	0.3400	0.1637	1.637	2	0.243	Supported	0.95
		Diff_3_4	3	0.0663	0.0060	0.1210	0.0577	1.991	2	0.185	Supported	1.15
		Diff_3_5	3	0.1317	0.0680	0.2320	0.0879	2.593	2	0.122	Supported	1.50
		Diff_4_5	3	0.0733	0.0070	0.1840	0.0965	1.317	2	0.319	Supported	0.76
		Diff_sum	3	1.0993	0.5610	1.4060	0.4677	4.071	2	0.055	Supported	2.35
		Diff_mean	3	0.1099	0.0561	0.1406	0.0468	5.037	2	0.055	Supported	2.91
	OmniCam	Diff_1_2	3	0.0163	0.0100	0.0210	0.0057	4.975	2	0.038	Not supported	2.87
		Diff_1_3	3	0.0887	0.0640	0.1100	0.0232	6.625	2	0.022	Not supported	3.83
		Diff_1_4	3	0.0447	0.0320	0.0670	0.0194	3.988	2	0.058	Supported	2.30
		Diff_1_5	3	0.0737	0.0230	0.1690	0.0826	1.544	2	0.262	Supported	0.89
		Diff_2_3	3	0.0987	0.0890	0.1100	0.0106	16.124	2	0.004	Not supported	9.31
		Diff_2_4	3	0.0303	0.0230	0.0420	0.0102	5.144	2	0.036	Not supported	2.97
		Diff_2_5	3	0.0450	0.0170	0.0980	0.0459	1.697	2	0.232	Supported	0.98
		Diff_3_4	3	0.0550	0.0390	0.0810	0.0227	4.194	2	0.052	Supported	2.42
		Diff_3_5	3	0.0553	0.0180	0.1160	0.0530	1.808	2	0.212	Supported	1.04
Diff_4_5		3	0.0170	0.0150	0.0200	0.0026	11.129	2	0.008	Not supported	6.43	
Diff_sum		3	0.5247	0.3650	0.7980	0.2378	3.821	2	0.062	Supported	2.21	
Diff_mean		3	0.0525	0.0365	0.0798	0.0238	5.037	2	0.062	Supported	2.91	

**Table 2.** t-test of the absolute differences (and the mean sum of the differences) of milled frameworks made by individual intra-oral scanners relative to the master model

Yellow represents the closest means to zero (thus the most accurate); blue represents accuracy within 10µm, and red represents the lowest standard deviation (thus the most precise)

Effect size (Cohen's d): Small = 0,2; Medium = 0,5; Large = 0,8

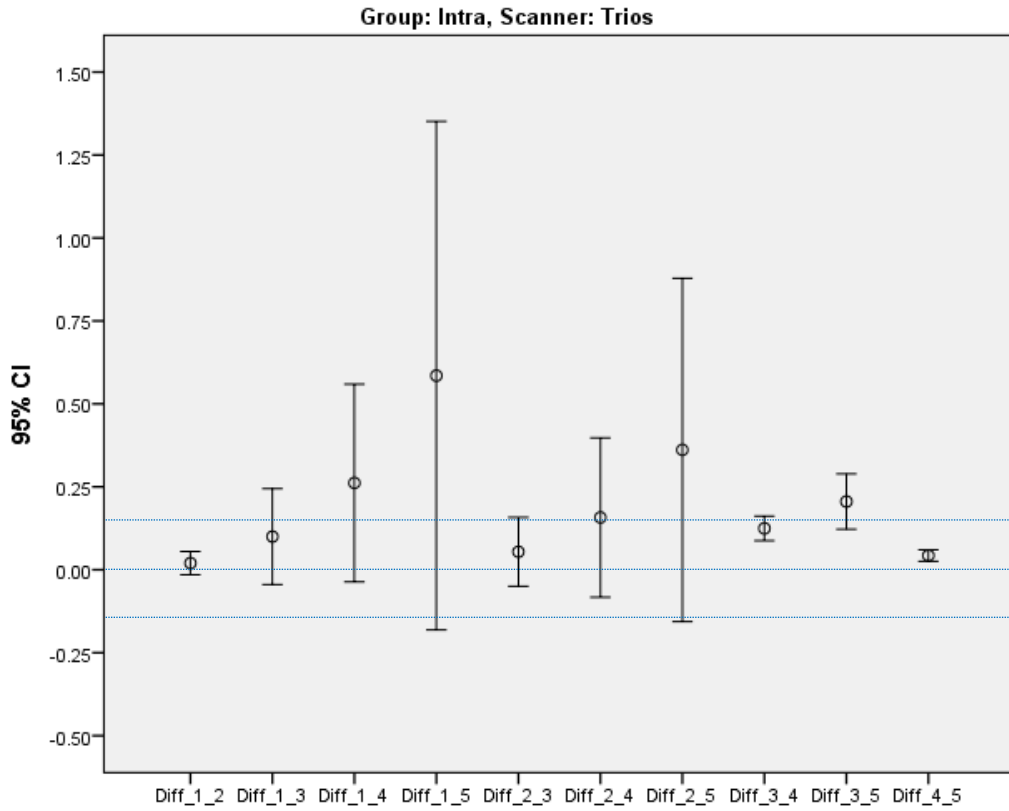


**Figure 4.1** Error bars of frameworks (created with the Trios® intra-oral scanner) relative to the master model at 95% confidence interval

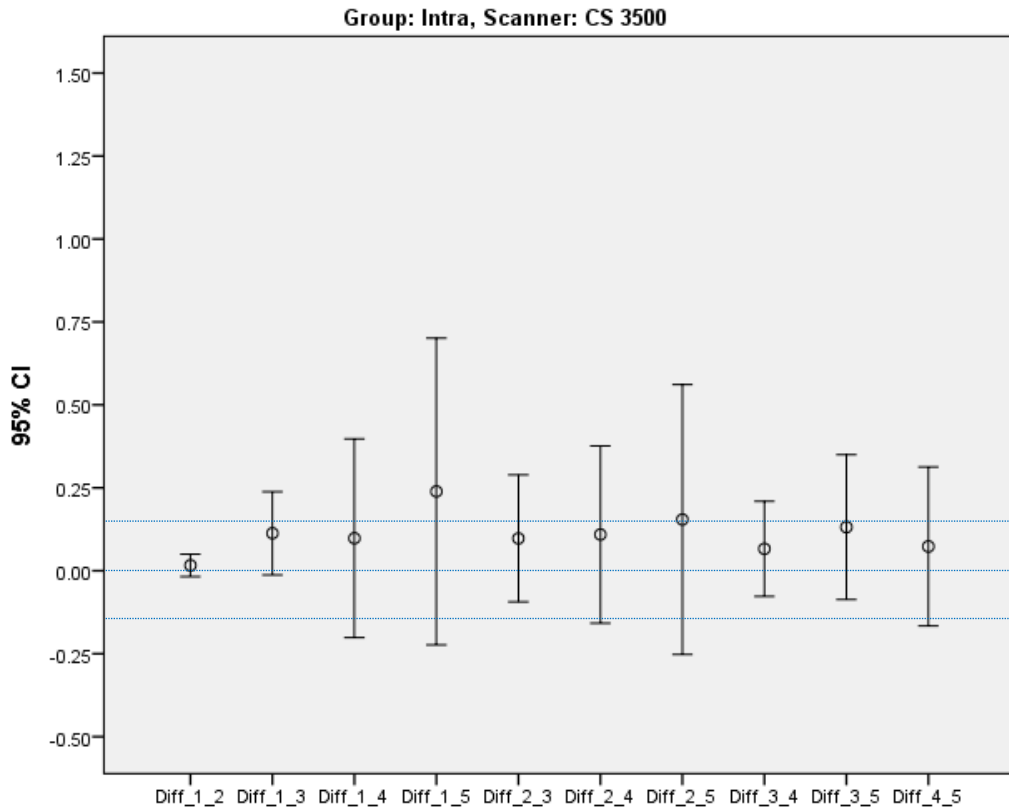


**Figure 4.2** Error bars of frameworks (created with the CS 3500 intra-oral scanner) relative to the master model at 95% confidence interval

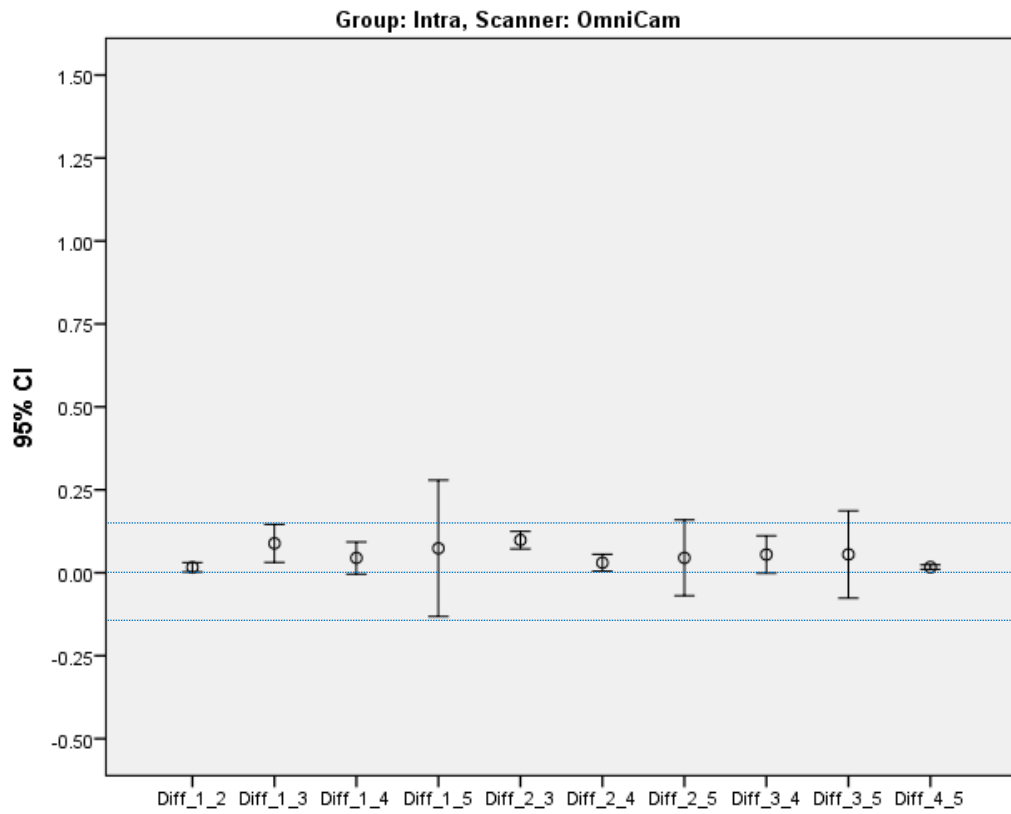


**Figure 4.3** Error bars of frameworks (created with the OmniCam intra-oral scanner) relative to the master model at 95% confidence interval

Group	Scanner	Distance	n	Mean	Min	Max	Std. Deviation	t	df	p-value	H0: Mean = 0	Effect size
Extra	D700	Diff_1_2	3	0.0430	0.0210	0.0790	0.0314	2.369	2	0.141	Supported	1.37
		Diff_1_3	3	0.0590	0.0400	0.0770	0.0185	5.518	2	0.031	Not supported	3.19
		Diff_1_4	3	0.0770	0.0680	0.0900	0.0115	11.564	2	0.007	Not supported	6.68
		Diff_1_5	3	0.0063	0.0010	0.0100	0.0047	2.321	2	0.146	Supported	1.34
		Diff_2_3	3	0.0417	0.0100	0.0680	0.0294	2.458	2	0.133	Supported	1.42
		Diff_2_4	3	0.0763	0.0510	0.0950	0.0227	5.813	2	0.028	Not supported	3.36
		Diff_2_5	3	0.0447	0.0220	0.0640	0.0212	3.650	2	0.068	Supported	2.11
		Diff_3_4	3	0.0740	0.0590	0.0940	0.0180	7.110	2	0.019	Not supported	4.10
		Diff_3_5	3	0.0557	0.0310	0.0690	0.0214	4.509	2	0.046	Not supported	2.60
		Diff_4_5	3	0.0307	0.0160	0.0460	0.0150	3.538	2	0.071	Supported	2.04
		Diff_sum	3	0.5083	0.4770	0.5300	0.0278	31.682	2	0.001	Not supported	18.29
		Diff_mean	3	0.0508	0.0477	0.0530	0.0028	5.037	2	0.001	Not supported	2.91
	inEos X5	Diff_1_2	3	0.0267	0.0180	0.0410	0.0125	3.694	2	0.066	Supported	2.13
		Diff_1_3	3	0.0187	0.0030	0.0470	0.0246	1.315	2	0.319	Supported	0.76
		Diff_1_4	3	0.0210	0.0040	0.0310	0.0148	2.458	2	0.133	Supported	1.42
		Diff_1_5	3	0.0597	0.0450	0.0740	0.0145	7.126	2	0.019	Not supported	4.11
		Diff_2_3	3	0.0390	0.0270	0.0500	0.0115	5.857	2	0.028	Not supported	3.38
		Diff_2_4	3	0.0233	0.0060	0.0390	0.0166	2.440	2	0.135	Supported	1.41
		Diff_2_5	3	0.0103	0.0020	0.0200	0.0091	1.972	2	0.187	Supported	1.14
		Diff_3_4	3	0.0147	0.0090	0.0240	0.0081	3.119	2	0.089	Supported	1.80
		Diff_3_5	3	0.0073	0.0020	0.0130	0.0055	2.306	2	0.148	Supported	1.33
		Diff_4_5	3	0.0280	0.0230	0.0320	0.0046	10.583	2	0.009	Not supported	6.11
		Diff_sum	3	0.2487	0.2180	0.2880	0.0358	12.032	2	0.007	Not supported	6.95
		Diff_mean	3	0.0249	0.0218	0.0288	0.0036	5.037	2	0.007	Not supported	2.91
	S600 ART	Diff_1_2	2	0.0160	0.0090	0.0230	0.0099	2.286	1	0.263	Supported	1.62
		Diff_1_3	2	0.0570	0.0260	0.0880	0.0438	1.839	1	0.317	Supported	1.30
		Diff_1_4	2	0.0110	0.0010	0.0210	0.0141	1.100	1	0.470	Supported	0.78
		Diff_1_5	2	0.0445	0.0350	0.0540	0.0134	4.684	1	0.134	Supported	3.31
		Diff_2_3	2	0.0585	0.0160	0.1010	0.0601	1.376	1	0.400	Supported	0.97
		Diff_2_4	2	0.0145	0.0090	0.0200	0.0078	2.636	1	0.231	Supported	1.86
		Diff_2_5	2	0.0430	0.0220	0.0640	0.0297	2.048	1	0.289	Supported	1.45
		Diff_3_4	2	0.0695	0.0280	0.1110	0.0587	1.675	1	0.343	Supported	1.18
		Diff_3_5	2	0.0430	0.0090	0.0770	0.0481	1.265	1	0.426	Supported	0.89
Diff_4_5		2	0.0310	0.0240	0.0380	0.0099	4.429	1	0.141	Supported	3.13	
Diff_sum		2	0.3880	0.3600	0.4160	0.0396	13.857	1	0.046	Not supported	9.80	
Diff_mean		2	0.0388	0.0360	0.0416	0.0040	5.037	1	0.046	Not supported	3.56	

**Table 3.** t-test of the absolute differences (and the mean sum of the differences) of milled frameworks made by individual extra-oral scanners relative to the master model

Yellow represents the closest mean to zero (thus the most accurate); blue represents accuracy within 10µm; green represents the best mean accuracy within 10 µm; red represents the lowest standard deviation (thus the most precise).

Effect size (Cohen's d): Small = 0,2; Medium = 0,5; Large = 0,8

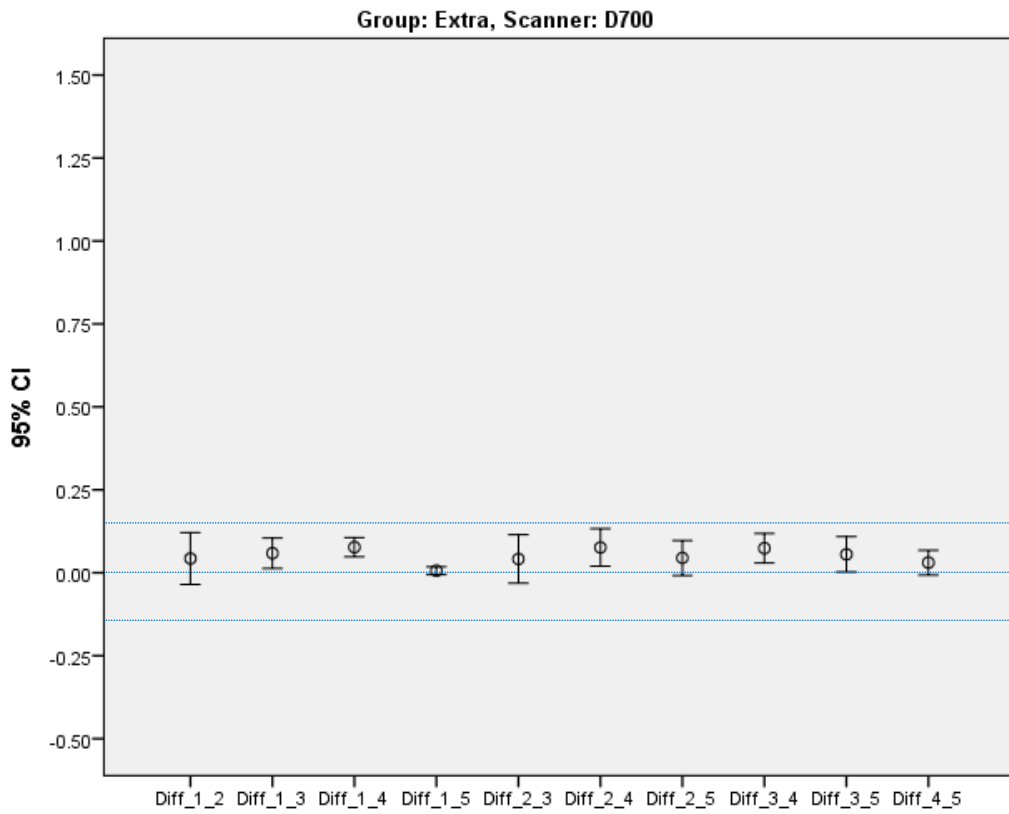


**Figure 4.4** Error bars of frameworks (created with the D700 extra-oral scanner) relative to the master model at 95% confidence interval

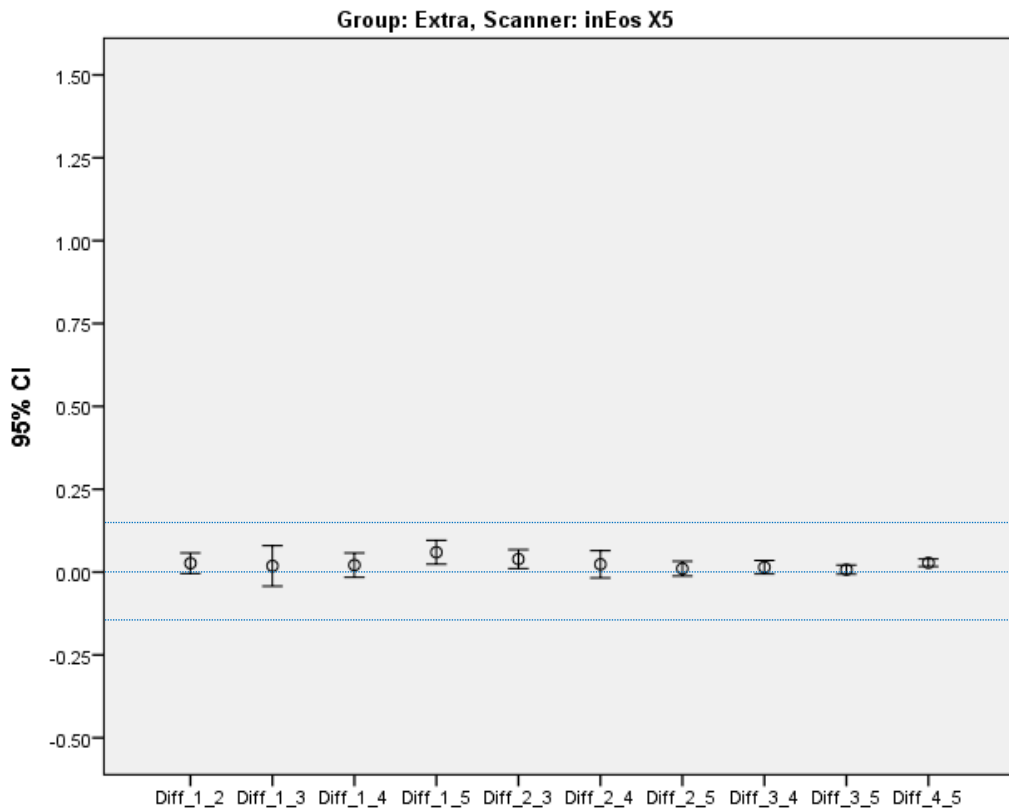


**Figure 4.5** Error bars of frameworks (created with the inEos X5 extra-oral scanner) relative to the master model at 95% confidence interval

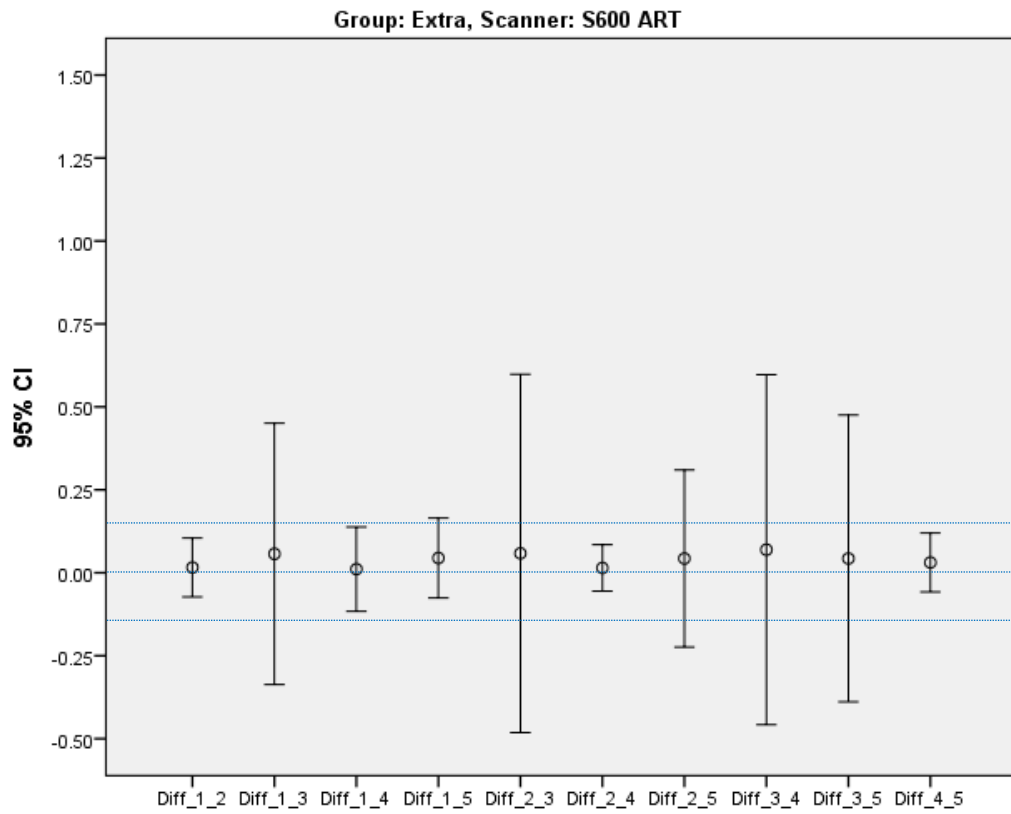


**Figure 4.6** Error bars of frameworks (created with the S600 ARTI extra-oral scanner) relative to the master model at 95% confidence interval

Group	Distance	n	Mean	Min	Max	Std. Deviation	t	df	p-value (2-tailed)	H0 (Mean = 0)*	Effect size
Intra	Diff_1_2	9	0.0176	0.0040	0.0310	0.0104	5.061	8	0.001	Not supported	1.69
	Diff_1_3	9	0.1006	0.0330	0.1700	0.0416	7.250	8	0.000	Not supported	2.42
	Diff_1_4	9	0.1348	0.0240	0.3490	0.1300	3.110	8	0.014	Not supported	1.04
	Diff_1_5	9	0.2992	0.0230	0.8780	0.2919	3.075	8	0.015	Not supported	1.03
	Diff_2_3	9	0.0836	0.0070	0.1790	0.0492	5.090	8	0.001	Not supported	1.70
	Diff_2_4	9	0.0991	0.0230	0.2470	0.0914	3.253	8	0.012	Not supported	1.08
	Diff_2_5	9	0.1870	0.0170	0.5760	0.1935	2.900	8	0.020	Not supported	0.97
	Diff_3_4	9	0.0820	0.0060	0.1410	0.0454	5.414	8	0.001	Not supported	1.80
	Diff_3_5	9	0.1309	0.0180	0.2440	0.0846	4.643	8	0.002	Not supported	1.55
	Diff_4_5	9	0.0444	0.0070	0.1840	0.0542	2.460	8	0.039	Not supported	0.82
	Diff_sum	9	1.1791	0.3650	2.5260	0.7363	4.804	8	0.001	Not supported	1.60
	Diff_mean	9	0.1179	0.0365	0.2526	0.0736	4.804	8	0.001	Not supported	1.60
Extra	Diff_1_2	8	0.0301	0.0090	0.0790	0.0218	3.913	7	0.006	Not supported	1.38
	Diff_1_3	8	0.0434	0.0030	0.0880	0.0311	3.950	7	0.006	Not supported	1.40
	Diff_1_4	8	0.0395	0.0010	0.0900	0.0333	3.353	7	0.012	Not supported	1.19
	Diff_1_5	8	0.0359	0.0010	0.0740	0.0270	3.755	7	0.007	Not supported	1.33
	Diff_2_3	8	0.0449	0.0100	0.1010	0.0295	4.297	7	0.004	Not supported	1.52
	Diff_2_4	8	0.0410	0.0060	0.0950	0.0332	3.490	7	0.010	Not supported	1.23
	Diff_2_5	8	0.0314	0.0020	0.0640	0.0241	3.679	7	0.008	Not supported	1.30
	Diff_3_4	8	0.0506	0.0090	0.1110	0.0387	3.705	7	0.008	Not supported	1.31
	Diff_3_5	8	0.0344	0.0020	0.0770	0.0316	3.077	7	0.018	Not supported	1.09
	Diff_4_5	8	0.0298	0.0160	0.0460	0.0093	9.047	7	0.000	Not supported	3.20
	Diff_sum	8	0.3809	0.2180	0.5300	0.1236	8.715	7	0.000	Not supported	3.08
	Diff_mean	8	0.0381	0.0218	0.0530	0.0124	8.715	7	0.000	Not supported	3.08

**Table 4.** t-test of the absolute differences (and the mean sum of the differences) of milled frameworks made by the group of intra-oral scanners and the group of extra-oral scanners relative to the master model

Yellow represents the closest mean to zero (thus the most accurate); blue represents the accuracy within 10µm; red represents the lowest standard deviation (thus the most precise)

Effect size (Cohen's d): Small = 0,2; Medium = 0,5; Large = 0,8

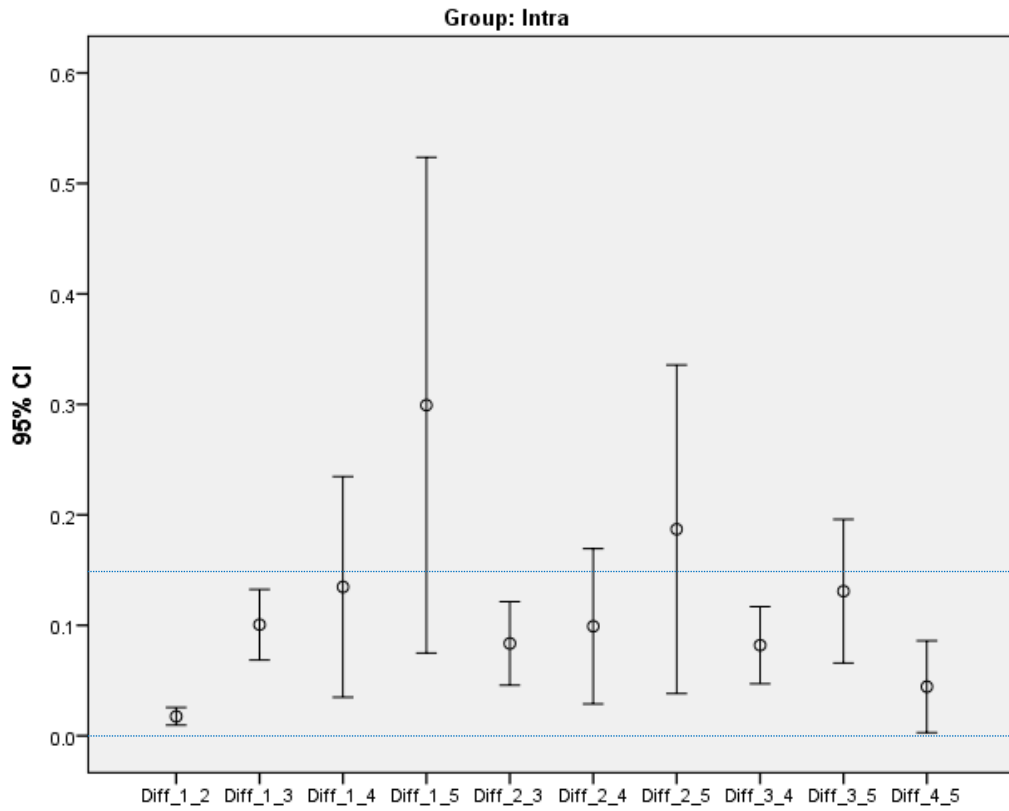


**Figure 4.7** Error bars of frameworks (created with the grouping intra-oral scanners) relative to the master model at 95% confidence interval

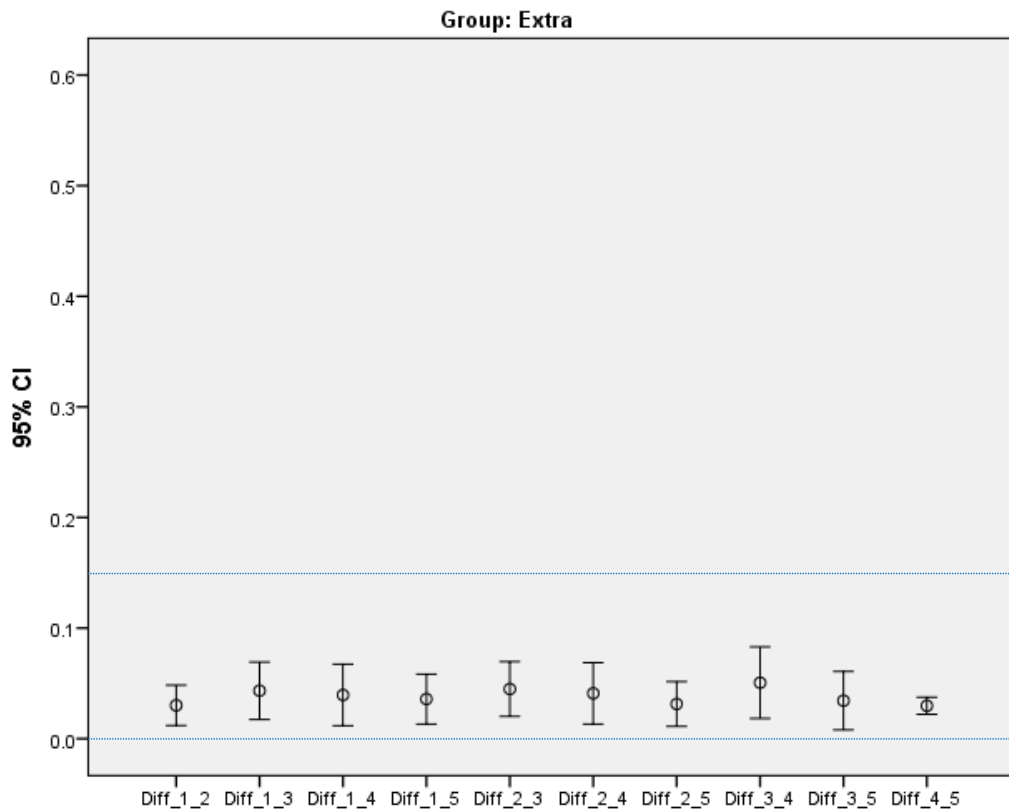


**Figure 4.8** Error bars of frameworks (created with grouping of extra-oral scanners) relative to the master model at 95% confidence interval

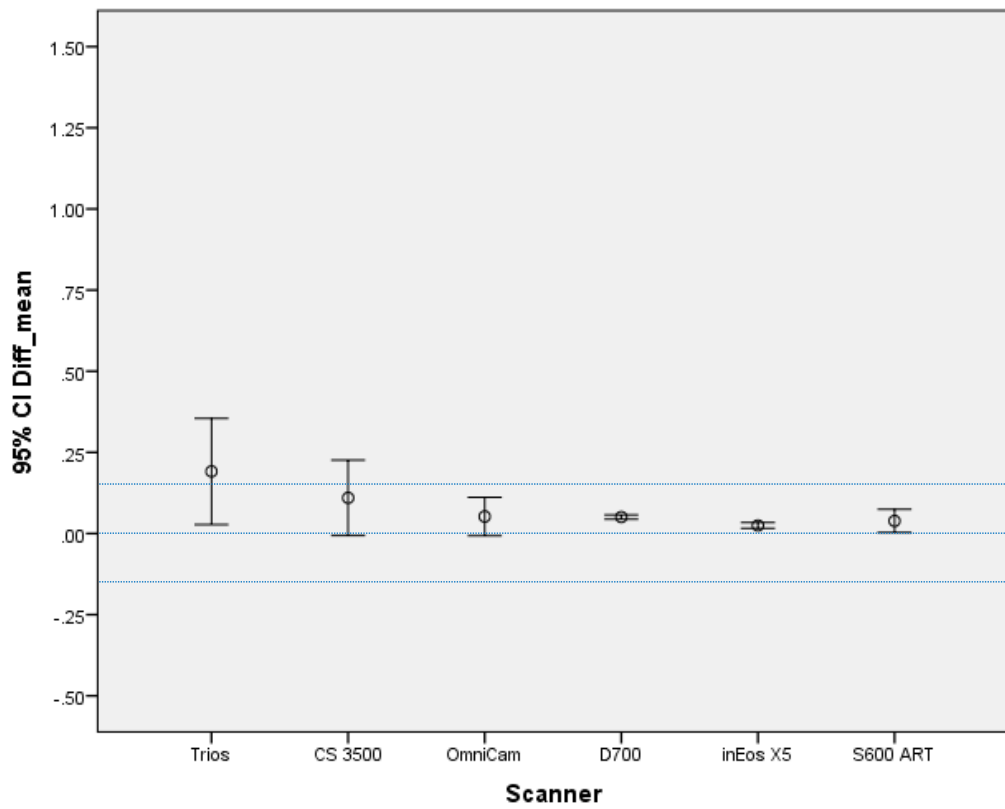


**Figure 4.9** Error bars of frameworks created with individual scanners using the mean sum of all measurements relative to the master model at 95% confidence interval

Distance	Group	n	Mean	Std. Deviation	Levene Statistic	Sig.	H0: Homogeneity of variance*	t	Sig.	H0: Equality of group means*	Effect size ( $\eta$ squared)
Diff_1_2	Intra	9	0.0176	0.0104	1.507	0.239	Supported	-1.549	0.142	Supported	0.13
	Extra	8	0.0301	0.0218							
Diff_1_3	Intra	9	0.1006	0.0416	0.562	0.465	Supported	3.175	0.006	Not supported	0.39
	Extra	8	0.0434	0.0311							
Diff_1_4	Intra	9	0.1348	0.1300	14.599	0.002	Not supported	2.121	0.062	Supported	0.22
	Extra	8	0.0395	0.0333							
Diff_1_5	Intra	9	0.2992	0.2919	13.727	0.002	Not supported	2.693	0.027	Not supported	0.31
	Extra	8	0.0359	0.0270							
Diff_2_3	Intra	9	0.0836	0.0492	0.659	0.430	Supported	1.930	0.073	Supported	0.19
	Extra	8	0.0449	0.0295							
Diff_2_4	Intra	9	0.0991	0.0914	12.127	0.003	Not supported	1.780	0.105	Supported	0.17
	Extra	8	0.0410	0.0332							
Diff_2_5	Intra	9	0.1870	0.1935	14.551	0.002	Not supported	2.393	0.043	Not supported	0.26
	Extra	8	0.0314	0.0241							
Diff_3_4	Intra	9	0.0820	0.0454	0.211	0.653	Supported	1.523	0.149	Supported	0.13
	Extra	8	0.0506	0.0387							
Diff_3_5	Intra	9	0.1309	0.0846	11.502	0.004	Not supported	3.183	0.009	Not supported	0.39
	Extra	8	0.0344	0.0316							
Diff_4_5	Intra	9	0.0444	0.0542	2.840	0.113	Supported	0.754	0.462	Supported	0.03
	Extra	8	0.0298	0.0093							

**Table 5.** t-test comparing intra-oral with extra-oral scanners using the absolute differences of milled frameworks relative to the master model

Yellow represents closest mean to zero (thus the most accurate); red represents the lowest standard deviation (thus the most precise)

Effect size ( $\eta$  squared): Small = 0,01; Medium = 0,06; Large = 0,14

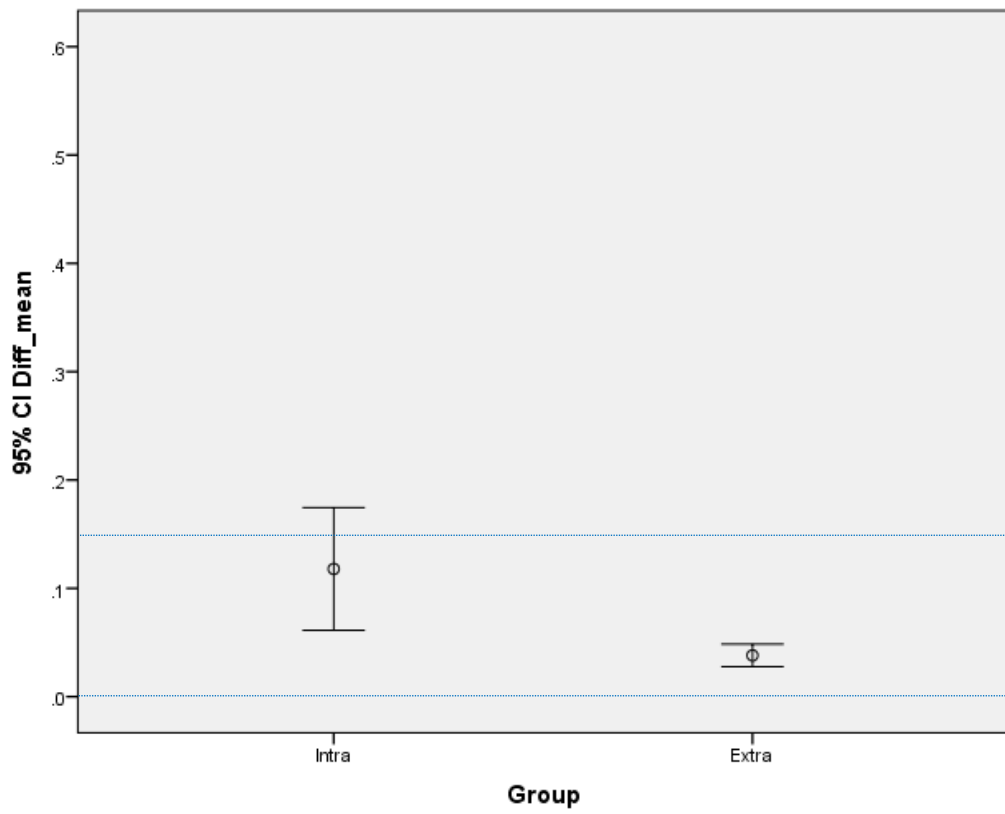


**Figure 4.10** Error bars of frameworks created with the intra-oral group of scanners and the extra-oral group of scanners using the mean sum of all measurements relative to the master model at 95% confidence interval

## CHAPTER 5. DISCUSSION

### 5.1 Discussion

One of the experiments (EXP 18) from the Zirkonzhan extra-oral scanner S600 ARTI (Zirkonzhan, Gais, Italy) was removed due to difficulty in stabilising the stainless-steel model within the scanner. The design of the clamps of this scanner is best suited for plaster models but the less secure stainless steel model was likely to have resulted in minor movements resulting in experimental errors. For this reason, experiment 18 was removed from the statistical analysis.

It is irrelevant whether there is expansion or contraction of the milled frameworks compared with the master model (i.e. the direction of misfit). Thus, the degree of misfit was determined as absolute differences to zero, where zero is the correlating measurement on the master model. The scanners were assessed on their accuracy for each of the ten distances measured per milled framework. In addition, the mean sum of the differences was calculated to give an overall accuracy of each scanner for its use in fabricating complete-arch implant-supported prostheses.

Even under the strict conditions of this study, producing a completely accurate framework was not possible. Analysis of the error bars (figures 4.1-4.6) provides important information on the accuracy of the scanners over varying distances. Where the standard deviation is low, there is a clustering of results which indicates reproducibility of the results over that distance. This must be considered with the mean values to determine accuracy relative to the master model. The effect size is large for the majority of statistical calculations indicating the certainty of the magnitude of the difference of mean values from zero.

For all the intra-oral scanners, there is a correlation between the standard deviation and the mean accuracy, and the distance scanned. The longer the length, the greater the standard deviation and the poorer the mean accuracy. This trend can be explained by the manner in which the scanners function. Smaller lenses at the end of a handheld scanner are guided along the arch (i.e. from point 1-2-3-4-5). Errors are thus compounded over greater distances.

The Sirona CEREC OmniCam exhibited the lowest standard deviation for all measurements and the most accurate mean for nine of the ten measurements, with the Carestream CS3500 having an equal mean accuracy for measurement 1-2 and being more accurate for measurement distance 2-3. The mean values of all the distances measured are above 10 $\mu$ m. Although all three intra-oral scanners were able to produce frameworks that had an accuracy of  $\leq 10\mu$ m for the shortest distance (1-2), this only occurred one out of three times for each scanner. The accuracy must be considered with the upper limits of the standard deviation to determine clinical acceptability. Based on Jemt's (1991) recommendation of a maximum permissible misfit of 150 $\mu$ m, this becomes the upper limit of the standard deviation. At a 95% confidence interval, the 3Shape Trios® was acceptable for distances 1-2 and 4-5. The Carestream CS3500 was only acceptable for distance 1-2. The Carestream intra-oral camera did not perform adequately at the similar distances of 2-3; 3-4 and 4-5. This makes its use unpredictable. The Sirona CEREC OmniCam was acceptable for distances 1-2; 1-3; 1-4; 2-3; 2-4; 3-4 and 4-5. Although this scanner was acceptable at distance 1-4, it was not acceptable at a similar distance 3-5.

For the extra-oral scanners, there is no correlation between the length of the measured distances and the accuracy of the milled framework. This is explained by the CNC method as the scans are taken with larger lenses capturing bigger images.

The Sirona CEREC Inlab inEos X5 showed the lowest standard deviation for five of the ten measurements, with the Zirkonzhan Scanner S600 ARTI for two of the measurements and the 3Shape D700 having the lowest for three of the measurements and the lowest mean standard deviation. This is indicative of how precise these scanners are but not how accurate. Due to the experimental loss for the Zirkonzhan Scanner S600 ARTI, the sample size decreased which meant a greater standard deviation. Statistically the comparison between other scanners must be interpreted with caution in figure 4.6, to assess the mean values as well as the maximum misfit. While the 3Shape D700 had a total mean accuracy of all distances of 51 $\mu\text{m}$ , the maximum misfit was 94 $\mu\text{m}$ . Similarly, the Sirona CEREC Inlab inEos X5 had a mean accuracy of 25 $\mu\text{m}$  with a maximum misfit of 74 $\mu\text{m}$ . The Zirkonzhan Scanner S600 ARTI had a mean accuracy of 39 $\mu\text{m}$ , but an upper limit of 111 $\mu\text{m}$ . All these scanners are within the recommended 150 $\mu\text{m}$  limit.

Figure 4.10 shows the statistically significant differences between the intra-oral and extra-oral scanners over a complete arch. The higher standard deviation evident with the group of intra-oral scanners indicates an undesired variation in results, thus a lower precision in achieving the mean compared with the extra-oral scanners. Furthermore, the upper limit of the standard deviation for the intra-oral scanners is beyond the recommended 150 $\mu\text{m}$  limit. However, when considering complete-arch implant-supported prostheses, the accuracy is determined by the range of misfit with the upper limit ultimately determining the extent (as seen in table 1).

When assessing intra-oral scanners for this purpose, the upper limits of misfit ranged from 169 $\mu$ m with the Sirona CEREC OmniCam up to 878 $\mu$ m with the 3Shape Trios®. None of the intra-oral scanners could therefore be recommended for complete-arch implant-supported prosthesis fabrication. The null hypothesis that there would be no difference in the accuracy of different scanning methods was therefore not supported.

## **5.2 Study limitations**

This study did not simulate oral conditions, thus the results would have to be interpreted with caution. It is uncertain whether the accuracy of intra-oral scanning is affected by patient movement or whether the accuracy of the scan is operator dependant.

In order to measure the pathway of the scanners, a milled structure was produced. This milling process itself may result in further discrepancies from the master cast. However, this does mimic the clinical scenario and the steps required to fabricate complete-arch prostheses.

## CHAPTER 6. CONCLUSION AND RECOMMENDATIONS

This is the first known study measuring the entire pathway for complete-arch implant prosthetics.

The milling of complete arch frameworks requires a degree of accuracy at all steps in the pathway to produce a clinically acceptable result. While the suggestion of 150 $\mu$ m is an acceptable limit, the evidence is not clear. There is little doubt that decreasing the misfit will result in a decrease of preload forces and thus stresses within the framework and therefore improved technical, biological and clinical outcomes (Estafanous, et al., 2016). Clinically, a more objective method is required to check the accuracy of the frameworks onto the master model. Perhaps the type of metrology used in this study may play a role in improving the fabrication of CAD/CAM frameworks in the pursuit of passivity.

The comparison between different models must be read with caution as developments in this field are rapid. For example, the new Trios® 3 (3Shape, Copenhagen, Denmark) intra-oral scanner and the new D1000 (3Shape, Copenhagen, Denmark) extra-oral scanner were not available at the time of the study.

Within the limitations of this study, for the intra-oral scanners, the 3Shape Trios® (3Shape, Copenhagen, Denmark) can be recommended for measurements up to 21,5mm and the Sirona CEREC OmniCam (Sirona Dental Systems, Inc., Bensheim, Germany) for measurements up to 34mm.

The extra-oral scanners used in this study have the appropriate accuracy as per Jemt (1991) for complete-arch implant prosthetics. As the accuracy of these is relative to the model or impression created, appropriate steps must always be taken to ensure the accuracy of the model (for example, the use of a verification jig).

There are many factors to consider when evaluating equipment of this nature, apart from accuracy and precision, such as the associated costs (initial outlay and maintenance), time efficiency, versatility and ease of use. Ideally, these factors should be combined and compared independently for each scanner upon release to guide clinicians and technicians in selecting the most appropriate for their desired use.

## REFERENCES

- Abduo J. Fit of CAD/CAM implant frameworks: a comprehensive review. *J Oral Implantol.* 2014; 40(6): 758-66
- Abduo J, Lyons K, Bennani V, Waddell N, Swain M. Fit of screw-retained fixed implant frameworks fabricated by different methods: a systematic review. *Int J Prosthodont.* 2011; 24(3): 207-20
- Adell R, Lekholm U, Rockler B, Brånemark P-I. A 15-year study of osseointegrated implants in the treatment of the edentulous jaw. *Int J Oral Surg.* 1981; 10(6): 387-416
- Astrand P, Ahlqvist J, Gunne J, Nilson H. Implant treatment of patients with edentulous jaws: a 20-year follow-up. *Clin Implant Dent Relat Res.* 2008; 10(4): 207-17
- Brånemark P-I. Osseointegration and its experimental background. *J Prosthet Dent.* 1983; 50(3): 399-410
- Brånemark P-I. *The Osseointegration Book: From Calvarium to Calcaneus.* Berlin ; Chicago: Quintessence Publishing Co Ltd. 2005
- Ekelund JA, Lindquist LW, Carlsson GE, Jemt T. Implant treatment in the edentulous mandible: a prospective study on Brånemark system implants over more than 20 years. *Int J Prosthodont.* 2003 16(6): 602-8
- Estafanous EW, Oates TW, Osswald M, Huynh-Ba G, Ellingsen J, Chvartzaid D. Thematic Abstract Review: Do We Get Improved Precision of Implant Fixed Dental Prostheses with Digital Scanners and Computer-Aided Design/Computer-Assisted Manufacture? *Int J Oral Maxillofac Implants.* 2016; 743–747
- Hexagonmi. Retrieved from hexagonmi: <http://www.hexagonmi.com/products/portable-measuring-arms/romer-absolute-arm-with-integrated-scanner>
- Hoods-Moonsammy VJ, Owen CP, Howes DG. A comparison of the accuracy of polyether, polyvinyl siloxane, and plaster impressions for long-span implant-supported prostheses. *Int J Prosthodont.* 2014; 27(5): 433-8
- Jemt T. Failures and complications in 391 consecutively inserted fixed prostheses supported by Brånemark implants in edentulous jaws: a study of treatment from the time of prosthesis placement to the first annual checkup. *Int J Oral Maxillofac Implants.* 1991; 6(3): 270-6
- Katsoulis J, Müller P, Mericske-Stern R, Blatz MB. CAD/CAM fabrication accuracy of long- vs. short-span implant-supported FDPs. *Clin Oral Implants Res.* 2015; 245-9
- Kim Y, Oh TJ, Misch CE, Wang HL. Occlusal considerations in implant therapy: clinical guidelines with biomechanical rationale. *Clin Oral Implants Res.* 2005; 16(1): 26-35

- Mitha T, Owen CP, Howes DG. The three-dimensional casting distortion of five implant-supported frameworks. *Int J Prosthodont.* 2009; 22(3): 248-50
- Papaspyridakos P, Chen CJ, Chuang SK, Weber HP, Gallucci GO. A systematic review of biologic and technical complications with fixed implant rehabilitations for edentulous patients. *Int J Oral Maxillofac Implants.* 2012; 27(1): 102-10
- Pjetursson BE, Asgeirsson AG, Zwahlen M, Sailer I. Improvements in implant dentistry over the last decade: comparison of survival and complication rates in older and newer publications. *Int J Oral Maxillofac Implants.* 2014; 29(Suppl): 308-24
- Sahin S, Cehreli MC. The significance of passive framework fit in implant prosthodontics: current status. *Implant Dent.* 2001; 10(2): 85-92
- Turkyilmaz I, Tözüm TF. 30-year Outcomes of Dental Implants Supporting Mandibular Fixed Dental Prostheses: A Retrospective Review of 4 Cases. *Implant Dent.* 2015; [Epub ahead of print].
- Vandeweghe S, Vervack V, Dierens M, De Bruyn H. Accuracy of digital impressions of multiple dental implants: an in vitro study. *Clin Oral Implants Res.* 2016; [Epub ahead of print].
- Zarb GA, Schmitt A. The longitudinal clinical effectiveness of osseointegrated dental implants: the Toronto study. Part III: Problems and complications encountered. *J Prosthet Dent.* 1990; 64(2): 185-94

## 7.1 Cited References

- Brånemark P-I, Hansson BO, Adell R, Breine U, Lindström J, Hallén O, Ohman A. Osseointegrated implants in the treatment of the edentulous jaw. Experience from a 10-year period. *Scand J Plast Reconstr Surg Suppl.* 1977; 16: 1-132. Cited in Turkyilmaz I, Tözüm TF. 2015. Not read in the original

## APPENDICES

### Appendix A

Ethics waiver

#### Human Research Ethics Committee (Medical)

Research Office Secretariat: Senate House Room SH10005, 10<sup>th</sup> floor. Tel +27 (0)11-717-1252  
Medical School Secretariat: Tobias Health Sciences Building, 2<sup>nd</sup> floor Tel +27 (0)11-717-2700  
Private Bag 3, Wits 2050, [www.wits.ac.za](http://www.wits.ac.za). Fax +27 (0)11-717-1265



Ref: W-CJ-151005-1.

05/10/2015

#### **TO WHOM IT MAY CONCERN:**

**Waiver:** This certifies that the following research does not require clearance from the Human Research Ethics Committee (Medical).

**Investigator:** Dr Michael Michael (student number 0306489H)

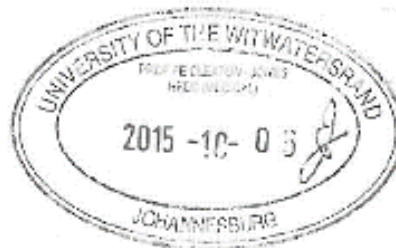
**Project title:** A comparison of the accuracy of different intra- and extra-oral digital scanners for milling an implant-supported framework.

**Reason:** This is a laboratory study. There are no human participants.

A handwritten signature in black ink, appearing to read 'Peter Cleaton-Jones'.

Professor Peter Cleaton-Jones

Chair: Human Research Ethics Committee (Medical)



Copy – HREC (Medical) Secretariat: Zanele Ndlovu.

## Appendix B

Plagiarism form: Turnitin report.

Similarity summary:

feedback studio | Writeupv5forTurnitin.docx | /0 | 1 of 7

### A Comparison of the Accuracy of Different Intra- and Extra-Oral Digital Scanners for Milling an Implant-Supported Framework

#### ABSTRACT

**Purpose:** To perform a comparative analysis of the accuracy of intra-oral and extra-oral digital scanners when used for the milling of a long-span implant supported superstructure framework.

**Method:** Three intra-oral and three extra-oral scanners were used to measure a master model containing five implant analogues. The three-dimension positions of the implant analogues were measured with a coordinate measuring machine. The digital data from the scanners were used to mill the implant positions in aluminium blanks from a single milling device. These implant positions were measured at the same points as the master model. The three-dimensional differences were calculated to provide a measure of the most accurate frameworks.

**Results:** For the intra-oral scanners, the further the measurement between points, the greater the standard deviation (the poorer the precision) and the poorer the mean accuracy. However, these were clinically acceptable over short distances. For the extra-oral scanners, there was no

#### Match Overview

**1%**

1	digital.lib.lehigh.edu Internet Source	<1%
2	www.hsas.ca Internet Source	<1%
3	file.scirp.org Internet Source	<1%

Similarity 1:

### CHAPTER 6. CONCLUSION AND RECOMMENDATIONS

This is the first known study measuring the entire pathway for complete-arch implant prosthetics.

The milling of complete arch frameworks requires a degree of accuracy at all steps in the pathway to produce a clinically acceptable result. While the suggestion of 150µm is an acceptable limit, the evidence is not clear. There is little doubt that decreasing the misfit will result in a decrease of preload forces and thus stresses within the framework and therefore improved technical, biological and clinical outcomes (Estafanous, et al., 2016). Clinically, a more objective method is required <sup>1</sup> to check the accuracy of the frameworks onto the master model. Perhaps the type of metrology used in this study may play a role in improving the fabrication of CAD/CAM frameworks in the pursuit of passivity.

## Similarity 2 (page 22)

For all the intra-oral scanners, there is a correlation between the standard deviation and the mean accuracy, and the distance scanned. The longer the length, the greater the standard deviation and the poorer the mean accuracy. This trend can be explained by the manner in which the scanners function. Smaller lenses at the end of a handheld scanner are guided along the arch (i.e. from point 1-2-3-4-5). Errors are thus compounded over greater distances.

## Similarity 3: (page 4)

With improved knowledge and technology, a number of approaches have been proposed to improve the fit of ISPs. A recent review on failure and complication rates in ISPs showed an improvement of outcomes in studies published in the last decade compared with prior studies (Pjetursson et al., 2014). This may partly be due to two different approaches, 1) the addition of fit refinement steps and 2) the elimination of fabrication steps. The first category includes techniques such as sectioning and soldering / laser welding frameworks. The second category includes computer-aided design/computer-assisted manufacturing (CAD/CAM) (Abduo et al., 2011). In their review, Abduo et al. (2011) concluded that CAD/CAM was able to provide the most consistent outcome.